

**EXPERIMENTAL STUDY OF ACID FRACTURE CONDUCTIVITY ON
SOFT CARBONATES**

A Thesis

by

YNGRID YRENE HORNICKEL VELASQUEZ

Submitted to the Office of Graduate and Professional Studies of
Texas A&M University
in partial fulfillment of the requirements for the degree of

MASTER OF SCIENCE

Chair of Committee, Ding Zhu
Committee Members, Daniel Hill
Yuefeng Sun

Head of Department, Daniel Hill

August 2017

Major Subject: Petroleum Engineering

Copyright 2017 Ynggrid Y. Hornickel Velasquez

ABSTRACT

Acid fracturing is a well stimulation technique used in carbonate formations. Its success relies upon the creation of conductive pathways that remain open after acid pumping stops. Through acid fracture conductivity experiments, it is possible to optimize treatment variables such as acid type, acid concentration, and flowrate.

In this study, eleven Kansas Chalk outcrops and four North Sea cores were tested for acid fracture conductivity. Both carbonate rocks are relatively soft. The feasibility of acid stimulation is investigated. The reaction of these rocks to straight 15% HCl, and to 15% HCl with corrosion inhibitor, surfactant, non-emulsifying agent, scale inhibitor and gelling agent, were analyzed. The variables in the experimental study include: temperature, acid type, acid concentration and contact time. These parameters were selected to mimic the field conditions. The acid tests were performed in a lab setup that reproduces these field settings. In order to quantify the volume of rock dissolved, the rock's surfaces were scanned before and after acidizing with a profilometer device. The created conductivity was measured for most samples at different closure stresses. In addition, porosity, Brinell Hardness, solubility tests, X-Ray Diffraction (XRD), X-Ray Fluorescence (XRF) and Scanning Electron Microscope (SEM) were performed on selected samples.

The results of this study show that including the aforementioned additives in the acid decreased the differential etching of soft carbonates. The effect was seen for both formations.

The North Sea cores developed a film on the fracture surface during the acid treatment. After analyzing portions of rock and residue, it was found that this insoluble material was mostly composed of quartz and some clay.

Differential dissolution of the North Sea cores was not observed. Therefore, poor conductivity from these cores was obtained under the experimented conditions. In addition, it was also noticed that increasing the contact time from 15 minutes to 25 minutes did not enhanced the resultant conductivity. Furthermore, for both formations, higher volume of rock dissolved did not result in higher conductivity.

The Kansas Chalk outcrop produced high conductivity at low closure stress when using straight acid, but it rapidly declined with increasing closure stress.

Based on the observed results, acid fracturing stimulation with the tested fluids is not recommended for the North Sea cores. The feasibility of using other methods to increase productivity should be investigated.

DEDICATION

To the memory of my beloved father;

To my mom, for her unconditional love;

To my kids, to show them that the sky is the limit;

To my dearly loved husband, for your constant support, your always wise words, your love, your jokes, your encouragement and your sweet and warm smile, even during my worst days. Thank you for believing in me more than anyone else. You are the BEST.

ACKNOWLEDGEMENTS

I would like to thank my committee chair, Dr. Ding Zhu and committee member Dr. Daniel Hill for giving me the opportunity to work in their research group and for their guidance throughout the course of this research. Also, I would like to thank Dr. Yuefeng Sun for being part of my committee and for his support during my time at Texas A&M.

I also want to express my gratitude to Igor Ivanishin for his contribution in the development of this project. His diligence, commitment and good attitude towards work made him the perfect teammate.

I would like to thank Jesse Guerra for his support and help to conduct the conductivity experiments. Your willingness to work in a project that you are not responsible for, was very meaningful to me.

I would like to thank John Maldonado for his support. He is an invaluable person in the department for those like me that are responsible for doing experimental work.

I also want to express my gratitude to Haoran Cheng, for his readiness to help when I needed it.

I want to thank Rachel Cash for her help and contribution towards the development of this project and for introducing me to the acid fracture conductivity tests.

Also, I would like to thank Assiya and Mateo for their encouragement and willingness to help.

Finally, thanks to my husband and kids for their patience and love.

CONTRIBUTORS AND FUNDING SOURCES

This study is supervised by Dr. Ding Zhu as the Committee Chair, and Dr. Dan Hill as the Committee member from Petroleum Engineering Department. They have guided the research direction and approach for the study. Dr. Yunfeng Sun as a Committee Member from Geology Department provided information about petroleum fluid flow in carbonate reservoir.

Igor Ivanishin as a fellow research contributed on conducting the experiments and analyze the experimental results.

The funding for the study was provided by ConocoPhillips.

TABLE OF CONTENTS

	Page
ABSTRACT	ii
DEDICATION	iv
ACKNOWLEDGEMENTS	v
CONTRIBUTORS AND FUNDING SOURCES.....	vi
TABLE OF CONTENTS	vii
LIST OF FIGURES.....	ix
LIST OF TABLES	xi
CHAPTER I INTRODUCTION AND LITERATURE REVIEW	1
1.1 Introduction.....	1
1.2 Literature Review.....	3
1.3 Stimulation of Soft Carbonates	10
1.4 Area of Study	11
1.5 Problem Description	12
1.6 Research Objective	13
CHAPTER II EXPERIMENTAL APPARATUS AND PROCEDURES	14
2.1 Brinell Hardness Measurement	17
2.2 Porosity Determination.....	19
2.3 Sample Preparation.....	19
2.4 Fracture Surface Characterization	23
2.5 Sample Saturation.....	25
2.6 Acid Injection	25
2.7 Fracture Conductivity Measurement	32
2.8 Solubility Test.....	42

CHAPTER III EXPERIMENTAL RESULTS AND DISCUSSION	43
3.1 Acid Etching Results	47
3.2 Solubility Tests and Analysis of Residual Material Results.....	60
3.3 Acid Fracture Conductivity Results	62
3.4 Discussion of Results.....	65
3.5 Comparison of Kansas Chalk and North Sea Chalk with Indiana Limestone.....	69
CHAPTER IV CONCLUSIONS AND RECOMMENDATIONS	72
4.1 Conclusions	72
4.2 Recommendations	73
REFERENCES.....	74

LIST OF FIGURES

	Page
Figure 1. Acid Fracture Conductivity Procedure	14
Figure 2. Sample Configuration	15
Figure 3. Steps for Sample Preparation.....	16
Figure 4. Mold for Sample Preparation.....	17
Figure 5. Brinell Hardness Equipment.....	18
Figure 6. Samples Configuration	20
Figure 7. Protection of Surfaces	21
Figure 8. Chalk and Sandstone Attachment	21
Figure 9. Cured RTV on Sample.....	23
Figure 10. Profilometer Reading.....	24
Figure 11. Vacuum Pump.....	25
Figure 12. Acid Fracturing Setup	26
Figure 13. API Modified Conductivity Cell.....	27
Figure 14. Sample Installation in Cell.....	28
Figure 15. Acid Setup Additions.....	29
Figure 16. RTV Sealant around Sample.....	30
Figure 17. Conductivity Test Setup.....	33
Figure 18. Sample Prepared for Conductivity Test.....	34
Figure 19. Lines Connected to Cell.....	36
Figure 20. Computation of Fracture Conductivity from Four Data Points	41
Figure 21. Surface Characterization of Sample #4. Right: Fracture Surface Scan from the Profilometer. Left: Picture of Acidized Fracture Surface.....	48

Figure 22. Acidized Surface of Sample #5.....	48
Figure 23. Surface Characterization of Sample #6. Right: Fracture Surface Scan from the Profilometer. Left: Picture of Acidized Fracture Surface.....	49
Figure 24. Surface Characterization of Sample #7. Right: Fracture Surface Scan from the Profilometer. Left: Picture of Acidized Fracture Surface.....	50
Figure 25. Surface Characterization of Sample #8. Right: Fracture Surface Scan from the Profilometer. Left: Picture of Acidized Fracture Surface.....	51
Figure 26. Surface Characterization of Sample #9. Right: Fracture Surface Scan from the Profilometer. Left: Picture of Acidized Fracture Surface.....	52
Figure 27. Surface Characterization of Sample #11. Right: Fracture Surface Scan from the Profilometer. Left: Picture of Acidized Fracture Surface.....	53
Figure 28. Acidized Fracture Surface of Sample # 12	54
Figure 29. Surface Characterization of Sample #13. Right: Fracture Surface Scan from the Profilometer. Left: Picture of Acidized Fracture Surface.....	56
Figure 30. Surface Characterization of Sample #14. Right: Fracture Surface Scan from the Profilometer. Left: Picture of Acidized Fracture Surface.....	58
Figure 31. Surface Characterization of Sample #15. Right: Fracture Surface Scan from the Profilometer. Left: Picture of Acidized Fracture Surface.....	59
Figure 32. Results from Solubility Test for Sample #12.....	60
Figure 33. SEM Result from Sample #13	62
Figure 34. Acid Fracture Conductivity Behavior.....	64
Figure 35. Brinell Hardness Relationship with Insoluble Material.....	69

LIST OF TABLES

	Page
Table 1. Parameters Used for Fracture Conductivity	41
Table 2. Experimental Conditions.....	44
Table 3. Summary of Experimental Results.....	46
Table 4. Acid Leakoff Weight vs Time for Sample #13	55
Table 5. Leakoff Measurement of Sample #14	57
Table 6. Leakoff vs Weight for Sample #15	59
Table 7. Results from Solubility Test, XRD, XRF and SEM Analysis	61
Table 8. XRF Results from Sample #15	62
Table 9. Results from Acid Fracture Conductivity Test	63
Table 10. Summary Results from Acid Fracture Conductivity Experiments	67

CHAPTER I

INTRODUCTION AND LITERATURE REVIEW

1.1 Introduction

Acid fracturing is a stimulation technique used in carbonate formations. During acid fracturing treatments, a viscous fluid known as “pad”, is first injected at a pressure above the fracturing pressure to initiate the fracture. Then, an acid system such as straight, gelled or emulsified acid is injected Beg et al. (1996). When the acid contact the fracture surfaces, it dissolves them. Heterogeneities of the rock creates non uniform reaction rates on the surface of the rock, generating uneven dissolution. This differential etching is expected to create conductive channels that remain open after the fracture closes, providing pathways for the fluid flowing from the formation to the wellbore.

The ability of flow in a fracture is measured by a parameter called conductivity. Fracture conductivity is defined as the product of fracture width with fracture permeability. The success of an acid fracturing treatment is associated with this retained conductivity after pumping stops.

Acid fracture conductivity can be determined experimentally. The conductivity test makes it possible to assess the variables that affect fracture conductivity such as, acid type, acid concentration, flowrate and contact time, to determine the optimum conditions

that reduces the weakening of the pillars created by the acid etching and allows for maximum flow capacity.

The created conductivity is influenced by the strength of the rock, the volume of rock dissolved, the created dissolution pattern and the closure stress (Pournik, 2008). The influence of these variables varies with closure stress. Initially, at low closure stress, the volume of rock dissolved and the dissolution pattern created have a major impact. If asperities are created on the fracture, conductive channels are formed. Conversely, a uniform dissolution along the fracture surface does not favor the creation of conductive channels for fluid flow. As closure stress increases, the created pillars need to sustain the overburden of the formation; therefore, rock strength has a major influence (Malagon, 2006).

Different etching patterns can be created on the fracture surface after acidizing, such as channeling and roughness dissolution. The created pattern is influenced by the characteristics of the rock (Pournik, 2008), as well as the acid system used (Pournik et al., 2010). A channeling pattern tends to preserve fracture conductivity longer; because channels are more difficult to crush (Melendez, 2007). While in a rough dissolution pattern, the retention of conductivity is influenced by the distribution of the asperities on the surface of the fracture (Antelo et al., 2009).

The selection of the acid system used for the treatment is dependent upon the reservoir characteristics. Most acid treatments use hydrochloric acid (HCl), but it instantly reacts with calcite; therefore, acid soluble polymers are added to the mixture to delay the reaction and reduce the fluid loss into the formation. In addition to the polymer, other

additives such as corrosion inhibitor, surfactants and scale inhibitor are added to the formulation. These additives alter the reaction between the HCl and calcite; thus, it is important to evaluate the fluid that is anticipated to be injected in the formation and determine the influence of these additives to the acid-rock interaction (Rabie and Nasr-El-Din, 2015) .

1.2 Literature Review

Acid fracturing is executed to improve well productivity in formations that are soluble in acid, such as limestone, dolomite and chalk formations. The conductivity reached after an acids job is considered as indication of a successful treatment. Several researchers have tried to understand all the parameters involved in the random interaction between rock and acid and the resulting conductivity. Different analysis on reaction rate, rock composition, closure stress, rock-acid contact time, acid type, rock embedment strength and acid fluid loss have been performed. The common approach to determine the effect of these parameters on conductivity is by experimental study.

Nierode and Kruk (1973) conducted a series of experiments where they studied the reaction of the acid with the fractured surface of carbonate rocks. They developed a correlation to predict conductivity. This correlation is strongly dependent on the amount of rock dissolved (DREC), the rock strength (RES) and formation closure stress, yet is independent of the heterogeneities of the rock. In addition, small core plugs were used to

perform the experiments (1 in by 2 in), which do not scale-up the roughness on the fracture faces observed in the field. Therefore, comparison of the acid fracture conductivity obtained with the Nierode and Kruk correlation and that from field measurements, indicate that Nierode and Kruk estimations can provide large errors. The correlation obtained from the researchers is shown below:

$$wk_f = C_1 \exp(-C_2 s) \quad (1.1)$$

$$C_1 = 0.265 (DREC)^{0.822} \quad (1.2)$$

$$C_2 * 10^3 = \begin{cases} 19.9 - 1.3 \ln(RES) & 0 < RES < 20,000 \text{ psi} \\ 3.8 - 0.28 \ln(RES) & 20000 \leq RES \leq 500,000 \text{ psi} \end{cases} \quad (1.3)$$

Deng et al. (2011) developed an intermediate scale correlation that fills up the gap between the grid size used in commercial fracture conductivity simulators and the size of core plugs in experiments. It ensures that small scale asperities and larger scale features such as channels, are captured. The correlation that predicts acid fracture conductivity is based on the modeling of the deformation of a rough fracture in heterogeneous formations. Such deformation is founded on the spatial distribution of permeability and mineralogy, from which the distribution of roughness and the resultant etching pattern after acidizing are determined. The correlation considers a base conductivity at zero closure stress and

the conductivity change with closure stress. The researchers used the same model used by Nierode et al. (1972), but with different constants (α , β):

$$wk_f = \alpha e^{-\beta \sigma_c} \quad (1.4)$$

These constants are calculated according to three different cases. Just the constants for the mineralogy distribution dominant case are presented.

1- Dominant permeability distribution, where is assumed that the mineralogy is homogeneous (100% calcite or dolomite), and the leakoff is higher than 0.004 ft/(min)^{0.5} or approximately 0.001 ft/(min)⁻⁵. Permeability effects prevail.

2- Dominant mineralogy distribution, where is considered that the mineralogy has a larger impact on the resulting etching pattern, and the leakoff is less than 0.004 ft/(min)⁻⁵. The percentage of calcite is considered to have the largest impact on fracture conductivity, and it is regarded through the term, $f_{calcite}$. The permeability distribution is not considered because is low. In **Equation 1.4**, the term α , incorporates the fracture conductivity at zero closure stress $(wk_f)_0$, which is calculated with the following equation:

$$(wk_f)_0 = 4.48 * 10^9 [1 + 2.97(1 - f_{calcite})^{2.02}] [0.13 f_{calcite}^{0.56}]^3 w_i^{2.52} \quad (1.5)$$

$$\alpha = (wk_f)_0 (0.811 - 0.853 f_{calcite}) \quad (1.6)$$

$$\beta = [1.2e^{0.952 f_{calcite}} + 10.5E^{-1.823}] * 10^{-4} \quad (1.7)$$

3- Competing effect of permeability and mineralogy distributions, where a medium leakoff coefficient is considered, about 0.001 ft/(min)⁵. The distribution of the permeability and the mineralogy affect the etching pattern and the resultant conductivity.

Anderson and Fredrickson (1989) created a procedure to determine fracture conductivity originated after an acid treatment. They stated that the factors that most influence acid etching and the created conductivity are the quantity of rock removed and the pattern of dissolution created. They believed that the kinetic parameters (acid type and strength, reaction temperature, time and flow regime) are responsible for the depth to which live acid penetrates while heterogeneous mineralogical composition enhances etching. They concluded that once etching is achieved, conductivity is governed by formation hardness and closure stress.

Studying the effect of the mineralogical composition of the rock, Van Domelen et al. (1992) stated that the etching pattern is influenced by the heterogeneity of the formation. In their experiments, it was established that a better etching is achieved when materials with different degree of solubility are present than when a uniform distribution exists. Likewise, they stated that reactive fluids produce higher leakoff than non-reactive fluids because of the formation of wormholes and the opening of the existing fractures. Another important conclusion they made in their research was that acid spending is not the factor that limits the effectiveness of an acid treatment but the fluid loss.

Beg et al. (1996) studied the influence of contact time and strength reduction as well as the effects of rock type and fluid loss. They observed that longer contact time is not always correlated to an increase in fracture conductivity, because as rock is exposed to the acid, it becomes weaker. Additionally, they found that when leakoff is included, the conductivity achieved is higher due to the increase in surface roughness. Furthermore, they established that the possibility of increasing the conductivity is higher when deep channels are created.

Gong et al. (1998) performed an experimental study to analyze the impact of acid etching and the weakening of the rock during an acid treatment, on the resultant conductivity. The researchers concluded that longer contact times results in rougher surfaces on the fracture face, in turn, higher fracture conductivity. Yet, the compressive strength of the rock is reduced causing the rough surface to easily crush under closure stress.

Melendez (2007) conducted a series of experiments using Indiana limestone, San Andres dolomite and Texas Cream chalk to study the relationship between acid contact time and rock strength to the resultant conductivity. She indicated that the creation of channels in the acidized rock dominate the behavior of the conductivity when closure stress is applied; while rock strength will be the dominant parameter when channels are not created. In addition, Melendez tested some outcrops from the North Sea. She found that these Samples had the lowest rock strength of all the tested rocks. Moreover, from the acid experiment a thin film covering the surface of the rock was observed which was believed to be preventive to the reaction. Not a defined etching pattern was observed.

The effect of acid etching on conductivity was previously studied by Pournik (2008). He concluded that there is an optimal contact time that will not reduce the conductivity created by the treatment. Such conductivity will be influenced by the formation and acid type as well as the temperature.

Considering that fluid loss is one of the major barriers in achieving an effective fracture penetration, different studies have been done on this subject.

Due to the importance of reducing acid leakoff rate and increase diversion, acid soluble polymers are usually added to increase the viscosity of the fluid. Thus, the efficiency of gelled acid on leakoff was studied by Bazin et al. (1999). They performed an experimental study using limestone cores, the fluids used were gelled HCl and straight HCl. They compared the velocities of wormhole propagation, leakoff volumes and dissolution pattern obtained from each acid and concluded that when using gelled acid, the surface roughness of the fracture faces is reduced and the leakoff fluid is also reduced by a factor ranging from 3 to 10, compared to the non-viscous fluid.

Narrowing down to the stimulation of chalk reservoirs, as soft carbonates; Mancillas et al. (1976) presented a paper where they explained the considerations made to stimulate Ekofisk field. Due to the thickness of the chalk, 42 wells were treated using the acid fracturing technique. To treat the wells, they used a mixture of hydrochloric acid and formic acid. Furthermore, particulate diverters were used to obtain a better distribution of the acid. They obtained favorable results and were able to increase considerably the productivity of all the wells.

While researching the Ekofisk field in the North Sea, Snow and Hough (1988) considered that the difficulty of the region to be stimulated lays primarily on the uniformity and softness of the massive chalk, which impedes the growth of the fractures and the generation of a differential etching that allows the formation of conductive paths. Additionally, they stated that the softness of the rock produce embedment of proppant and the collapse of the created fractures.

Cook and Brekke (2002) studied the productivity preservation in hydraulic propped fractures and based their research on chalk fields from the North Sea. They stated that at short term, acid fracturing is a good stimulation method but in the medium term the production tends to decline. They attributed this behavior to the typical characteristics of chalks: low hardness and homogeneity.

Lindgreen et al. (2012) studied the effect of mineralogical composition on the reservoir properties of the Ekofisk formation (chalk). They used samples from three different wells, differentiating them in clay-poor and clay-rich horizons. They characterized the chalk in terms of porosity and permeability. Additionally, the samples were analyzed with X-ray diffraction and atomic force microscope. They found that the chalk matrix contains a large amount of non-calcite material and about $2/3$ of this residue is nano-quartz. The authors found that the content of nano-quartz and clay minerals affect the porosity.

1.3 Stimulation of Soft Carbonates

Soft carbonates, such as chalks, are challenging to stimulate. They are characterized for being massive and uniform structures that produces short fracture length (Snow and Hough, 1988). They also have low hardness and a ductile behavior that favors pore collapse. Known for being homogeneous rocks, more even etches are observed on the fractured surface during acid treatments in chalks. As effective stress increases, creep failure follows on the face of the fracture; sometimes it could lead to complete fracture closure (Mader, 1989). Therefore, stimulation treatments have to be designed to economically produce a low permeability and fragile chalk formation. Some studies suggest the use of acid fracturing (Snow and Hough, 1988, Bocaneala et al., 2015) because all the screen out problems created by proppant. Others claim that, contrary to acid treatments that have an instantaneous reaction with the rock, proppant promotes deeper fractures and longer term production (Cook and Brekke, 2004). (Abass et al., 2006). Other researchers recommend the use of the Brinell Hardness Number (BHN) as a reference to distinguish between proppant and acid fracturing; being “soft chalk” ($BHN < 10 \text{ kgf/mm}^2$) better candidates for proppant and “hard chalk” ($BHN > 10 \text{ kgf/mm}^2$) more suitable to undergo acid treatments (Gistau, 1985).

There is not a quantitative method that standardize the use of one method over the other. The swap between acid fracturing and propped fractures has centered in the goal of productivity preservation and economic consideration.

1.4 Area of Study

In this research, the samples studied belong to two different formations: Kansas Chalk and North Sea Chalk. Most chalks around the world were formed during the Cretaceous period, which was a time of high sea levels, warm waters and a large production of coccoliths. The accumulation of the skeletons of these microorganisms on the ocean floor, formed chalk sediments (Van der Voet, 2015).

1.4.1 Kansas Chalk

Kansas Chalk belongs to the Niobrara Formation. The chalks in this region were formed from the accumulation of coccoliths from microorganisms living in the Western Interior Seaway; which was an inland that divided the continent of North America during the Cretaceous period. The sediments present are mostly from pelagic origin, with some contribution of terrigenous sources. Usually chalks are deposited in deep water environments at low sedimentation rates, but in the Niobrara formation chalks are considered unpure and were deposited in shallow sea water during a period of extensive volcanic activity. These rocks can have some dolomite in amounts up to 6 wt% and insoluble materials present are mainly clay minerals and quartz with minor amounts of feldspar and pyrite (Pollastro and Martinez, 2012).

1.4.2 North Sea Chalk

The chalk in the North Sea were formed by the increase in the sea level caused by the transgression in Northwest Europe. Flooding and lack of terrigenous material into the

ocean resulted in an increase in the production of coccoliths, which accumulated in the ocean floor and formed the “Chalk Group”. Insoluble materials present in the area are associated with the presence of radiolarian microorganisms; whose skeletons turned into amorphous silica after dissolution and reprecipitation (Maliva and Dickson, 1992).

1.5 Problem Description

Chalk reservoirs present a challenge for stimulation. Its low permeability, homogeneity, low hardness and ductile behavior contributes to evenly etched, short and radial fractures, as well as pore collapse and fracture closure. Therefore, engineers are constantly looking for the best practices that allows them to reach the highest productivity from each well. Lab scale experiments permits (1) optimize the treatment variables (acid type, contact time, acid concentration, pumping rate), (2) study the interactions and reaction products (if any) that occur when a particular acid system reaches the surface of the rock, (3) estimate the resulting conductivity at different closure stress. Knowledge of these parameters also prevents the implementation of fluids that are not compatible with the mineralogy of the formation and that otherwise could cause the loss of the well.

1.6 Research Objective

The purpose of this research is to identify the factors that affect the resulting conductivity of soft carbonates. Chalk outcrops and field core samples, are used to carry out the analysis.

The main objectives of the study are:

- 1- To perform acid fracture conductivity experiments with soft carbonate rocks (Kansas Chalk outcrops and North Sea Chalk cores).
- 2- To analyze the difference in the acid fracture conductivity experiments of soft carbonates from different formations.
- 3- Determine the feasibility of performing acid treatments on the North Sea cores with the proposed acid system.

CHAPTER II

EXPERIMENTAL APPARATUS AND PROCEDURES

To conduct the acid fracture conductivity experiments and the rock characterization, different procedures and equipment were used. For acid fracture conductivity we followed the process showed in **Figure 1**.

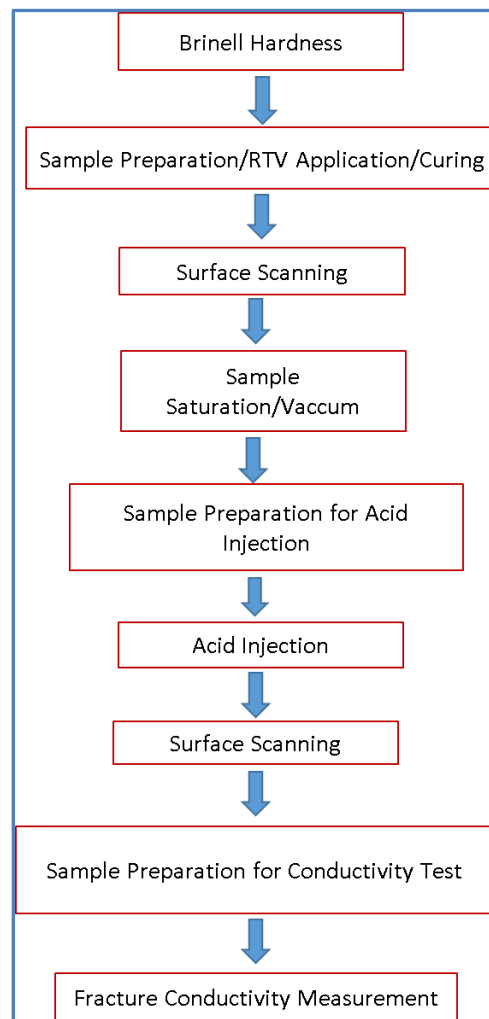


Figure 1. Acid Fracture Conductivity Procedure

Each acid fracture conductivity takes two pieces of rock samples. The two pieces are put together with a fracture in between. The fracture width is previously defined (**Figure 2**). In this case, a fracture width of 0.2 in was established.

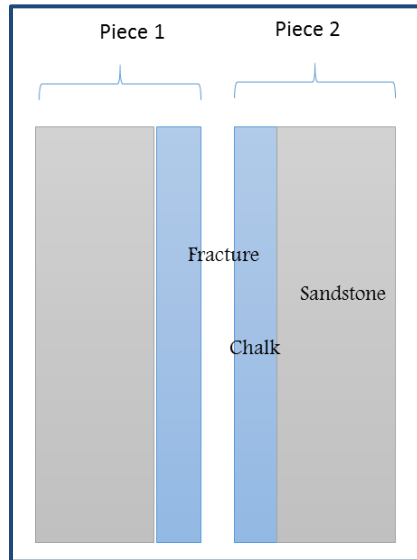


Figure 2. Sample Configuration

Because the downhole core supply was limited, the experiments were expected to be done using cores with a thickness of 0.45 in. When using these samples, it was observed that the rocks broke easily; therefore, it was necessary to increase the thickness of the chalk to 0.9 in. To prevent further breakage, the procedure for sealing the cores with RTV (Room Temperature Vulcanization) silicone was reduced from three steps to one step, with longer curing time. In previous experiments, the first stage was poured and let it dry; then, a second stage was poured on top of the previously dried RTV and also it let dry. Finally, a third stage of RTV was poured on the top of the previous one to complete the

process (**Figure 3, upper**). With the new procedure, a longer mold was used to place the RTV in just one stage, as shown in **Figure 3, bottom**.

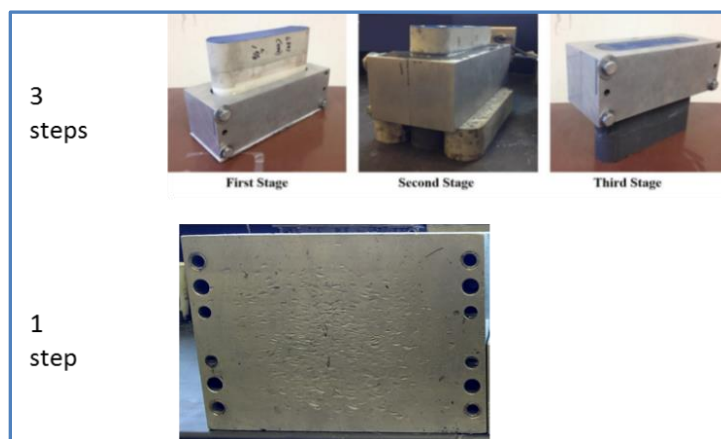


Figure 3. Steps for Sample Preparation

Even with this prevention mechanisms; it was witnessed that some samples still broke when placed or extracted from the curing mold. Therefore, chalk thickness was increased to 1.2 in. At this width, the sample integrity was maintained and then, it was possible to use the mold shown in (**Figure 4**), whose dimensions guaranteed a better seal between the sample and the acid cell; thus, leakoff measurements could be achieved.

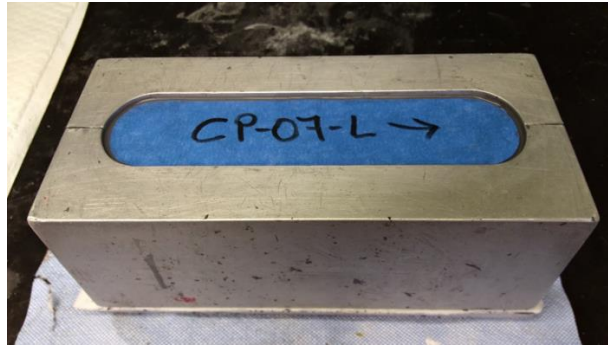


Figure 4. Mold for Sample Preparation

2.1 Brinell Hardness Measurement

The hardness of a material refers to its resistance to permanent indentation. In the case of rocks, it is related to its properties (mineralogy, density, anisotropy, degree of saturation, point load strength, etc.). The level of rock strength is directly related to the ability of the rock in sustaining conductivity after an acid treatment.

Different hardness tests have been developed, one of them is the Brinell Hardness, which is defined in ASTM E10. In this test, the hardness value is obtained by using a fixed force to push a given indenter into the rock surface. Smaller indentations indicate harder materials.

The Brinell Hardness test, was done using a GCTS Point Load Test System PLT-100, as shown in **Figure 5, left**.

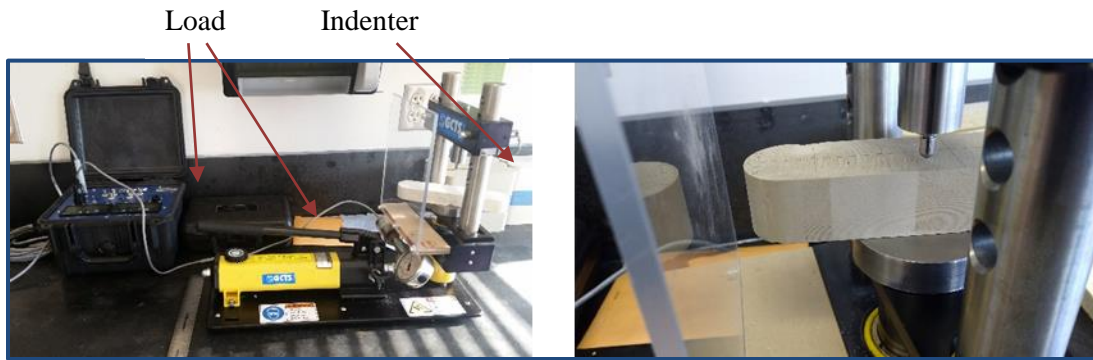


Figure 5. Brinell Hardness Equipment

To perform this test, the sample is divided into sections (**Figure 5, right**), that denote the places where the Brinell Hardness measurements are taken. Then, the indenter of the equipment is brought into contact with the sample in a direction perpendicular to the surface. Next, a test force is applied for 10 to 15 seconds and then removed. For these experiments, a standard size indenter of 3.175 mm was used; also two loads were applied, one of 0.15 KN and another one of 0.25 KN.

After the measurements have been taken, the following relationship is used to calculate the Brinell Hardness number (BHN):

$$BHN = \frac{L}{\left(\frac{\pi D}{2}\right)(D - \sqrt{D^2 - d^2})} \quad (2.1)$$

where D is the diameter of ball indenter (mm), d: is the diameter of indentation (mm) and L is the applied load (kgf).

2.2 Porosity Determination

The porosity (\emptyset) of the samples was calculated theoretically by volumes and by densities, as shown in equation 2.2 and 2.3.

$$\emptyset = \frac{\text{Pore Volume}}{\text{Total Volume}} * 100 \quad (2.2)$$

$$\emptyset = \frac{\text{Rock Density} - \text{Grain Density}}{\text{Grain Density}} * 100 \quad (2.3)$$

2.3 Sample Preparation

The samples are cut to the required thickness and to the proper size that fits the acid cell (7 in length x 1.61 in width in x 1.2 in thick). Every piece of chalk is matched with a piece of sandstone of equal length and width and a thickness of 1.8 in, to fit the dimensions of the acid cell. The samples shape and dimensions are shown in **(Figure 6)**.

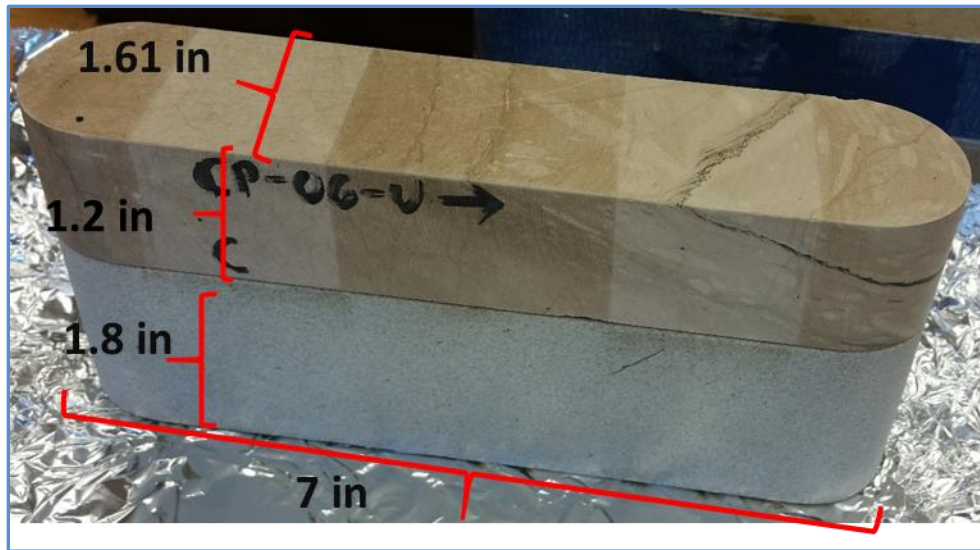


Figure 6. Samples Configuration

The following procedure was used to prepare the samples:

For the North Sea cores, weight the pieces of chalk and place them in the oven for a period of 24 hours at 110 °F. Weight them again, and record the weight loss.

For both rocks (Kansas Chalk outcrop and North Sea core):

- 1- Cover top and bottom of each sample with painter's tape, to protect their surface (**Figure 7**).

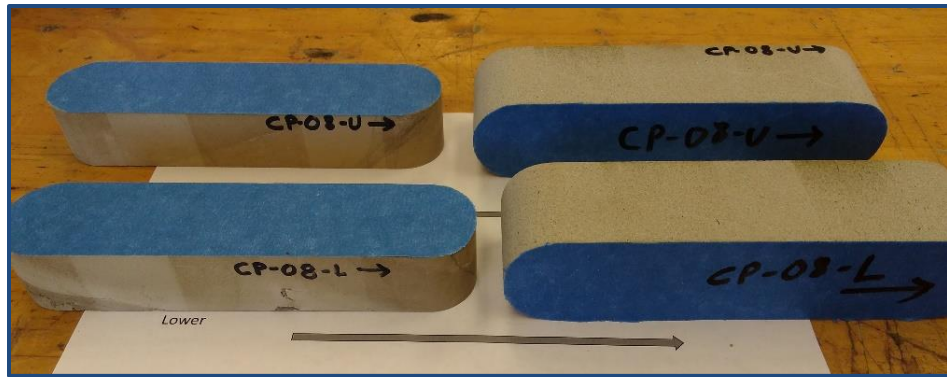


Figure 7. Protection of Surfaces

- 2- Attach together the chalk and the sandstone with painters tape. Do not use glue as it enhances the possibility of breakage by uneven surface between both rocks (**Figure 8**).

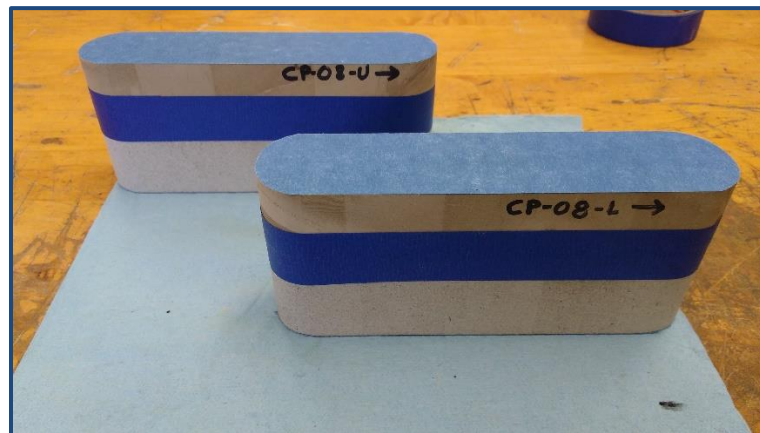


Figure 8. Chalk and Sandstone Attachment

- 3- Apply three layers of primer (Momentive SS4155) to the samples. This fluid helps promote adhesion between the rock and the RTV. It is necessary to wait until the primer dries between each application (about 10 minutes).
- 4- Apply three layers of silicon mold and also smear some grease on the edges of the mold to prevent leakage. It was important to remove the excess of grease since it alters the proper functioning of the silicon and also interacts with the RTV.
- 5- Place the cores inside the mold and pour Momentive RTV 627, which has been prepared by mixing it in a ratio of 1:1, 70 grams of each compound. Slowly and with the help of a syringe, inject the mixture in the gap between the mold and the rock. The purpose of this material is to create a seal between the sample and the cell. The sample must be centric in the mold by the end of the process, thus the resulting coating is evenly distributed around it.
- 6- After an hour of pouring the RTV, fill up the reduced level of compound, due to material settling. Remove the protective blue painters tape from the surface of the rock to prevent the glue from the tape to stick to the sample.
- 7- Allow sample to dry at room temperature for a period of 30 hours.
- 8- Disassembled the mold by removing the bottom part and all the screws. Carefully and with the help of an exacto knife, detach the RTV from the mold at the top and the bottom of the sample. The sample can now be carefully extracted from the mold (**Figure 9**).



Figure 9. Cured RTV on Sample

- 9- Bevel the edges of the sample with an exacto knife, top and bottom; to facilitate its placement into the acid cell.
- 10- Samples are ready to be scanned.

2.4 Fracture Surface Characterization

The surface of both samples are scanned before and after running the acid. The objective of this procedure is to obtain a matrix of values that later is used to calculate the volume of rock dissolved by the acid and also to characterize the etching patterns created by the acid solution. The device used to carry out the surface characterization is a profilometer. This device has a laser sensor that measures surface variations as a function of position.

To perform this assessment, the sample is placed in a movable table with the surface to be scanned facing up while the laser sensor measures the surface variations. The settings desired to carry out the scan are typed into the software that controls the equipment. The parameters introduced are the length of the sample (7 in), the width to scan (1.7 in) and the horizontal X and Y scan resolution, which is set to 0.05 in (**Figure 10**). The resolution of the vertical measurement is set to 0.002 in. The sample is scanned several times until the width (1.7 in) and length (7 in) introduced in the settings are completed. It takes about 3 hours to perform the surface characterization of each piece of sample.

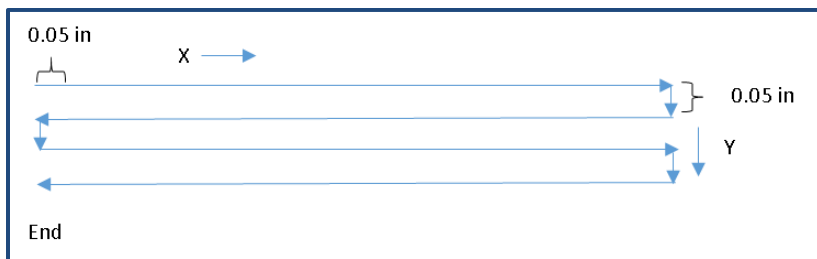


Figure 10. Profilometer Reading

The software that controls the profilometer generates a file that is hosted in a program created in Matlab (Malagon, 2006). From this program, we obtain the volume of rock dissolved from each side of the sample and 3-D images of the surfaces of the sample that give us an insight of the etching patterns created by the acid.

2.5 Sample Saturation

Samples are placed for 4 hours in a glass vessel connected to a vacuum pump. This procedure saturates the pores of the rock with water. **Figure 11** shows the equipment used.



Figure 11. Vacuum Pump

2.6 Acid Injection

The apparatus for acid injection developed by Zou (2006), was modified to increase the precision of fracture width and to enhance the safety of this research. The main components of the set up are the API modified conductivity cell, pump, acid storage

tank, water storage tank, heating tape, heating jacket, nitrogen tanks, cell pressure transmitter, differential pressure transmitter, thermocouple, heavy duty frame (to support the cell) and spent acid tank (**Figure 12**).

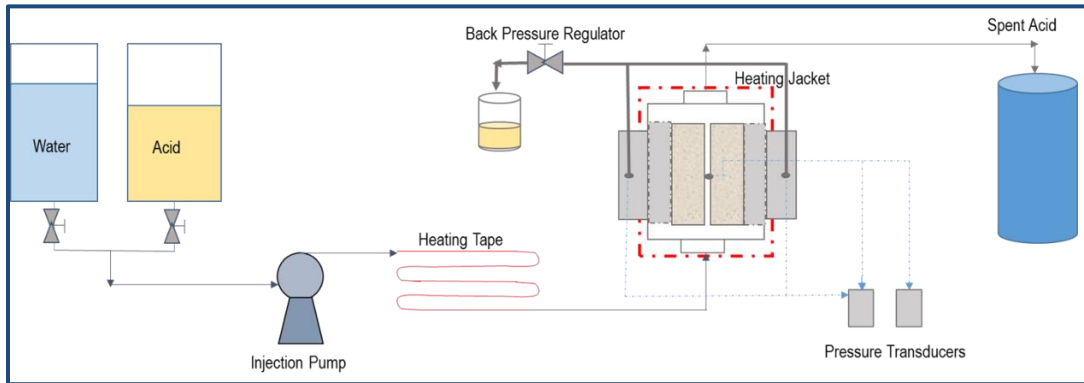


Figure 12. Acid Fracturing Setup

The cell is made of Hallsteloy, a corrosion resistant material. It is a modification made to the conductivity cell Petroleum (1989). It has a block shape body of dimensions 10'' x 3 ¼'' by 8'' with a rectangular hole with round edges in the center of dimensions 7 ¼'' by 1 ¾'', where the samples are placed. In the setup, the cell is placed in a vertical position to avoid gravity effects. Inside the cell, there is a groove where an O-ring (75-VITON-252) is located. This element is very important to control leakoff. The samples are kept inside the cell by two side pistons, which are also retained in place by the heavy duty frame and locked with two long screws. Viton O-rings (2-VITON-351) are also installed in the side pistons to create a seal and prevent fluid leakage. The acid cell also has flow inserts to connect it to the inlet and outlet flow lines (**Figure 13**).

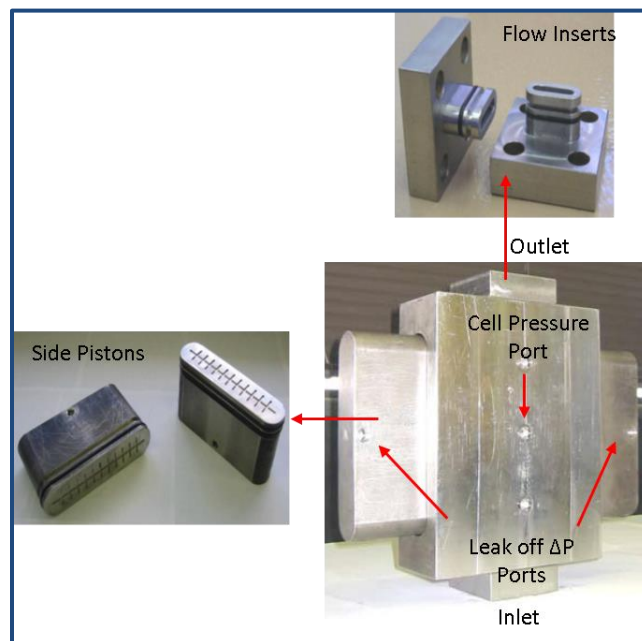


Figure 13. API Modified Conductivity Cell

The cell has three pressure ports. There is one pressure port in each side piston; they are connected to pressure transducers. The middle port from the body monitors the pressure in the cell, while the ports in the side pistons together with the middle cell port, are used to monitor the differential pressure to allow for fluid leakoff. This leakoff fluid can be collected through a leakoff line.

The system is connected to two nitrogen tanks. One of the tanks pressurizes the cell to 1000 psi with the use of a back pressure regulator. At this pressure the CO₂ resulting from the reaction between the HCl and calcite remains dissolved. The other nitrogen tank has also installed a back pressure regulator that keeps the pressure at a specified lower

setting to establish the pressure differential required to obtain the leakoff fluid through the leakoff line. In this case, the pressure differential was set to 20 psi.

When the two pieces of the samples are introduced into the cell, they are separated by a gap that corresponds to an artificial fracture, which is carefully maintained using a Teflon shim. For these experiments, a fracture width of 0.2 in is used (**Figure 14**).

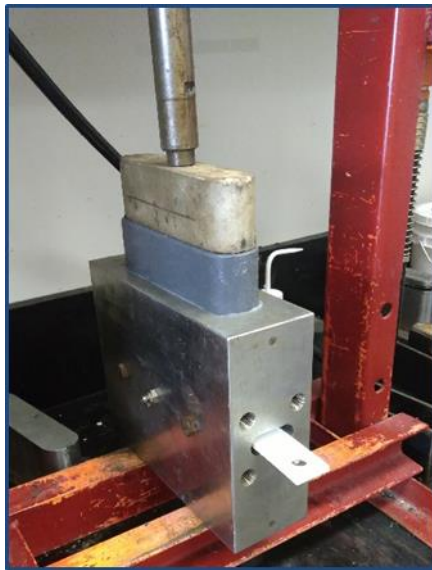


Figure 14. Sample Installation in Cell

In addition, the heavy duty frame where the acid cell is placed during an acid test, was modified to improve the precision of the fracture width and safety during the experiments. As shown in **Figure 15**, two metallic toppers prevent the side pistons from going further inside the cell, while the pistons are being installed. Also, a safety element located at the bottom of the cell prevents its movement during the tests.

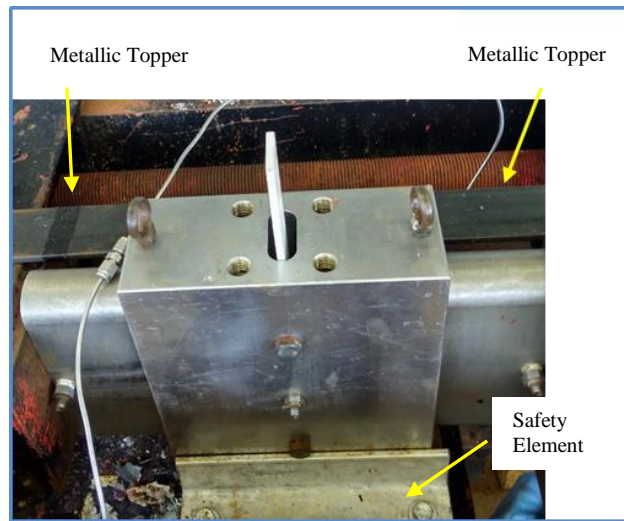


Figure 15. Acid Setup Additions

The setup has installed a heating tape and a thermocouple in the outlet of the cell to keep control of the temperature of the fluid temperature. In this case, the temperature is set to 100 °F.

The temperature of the rock is also controlled using a heating jacket; the rock temperature is set at 150 °F. It takes about 6 hours to reach this temperature.

Before initiating the acid injection, the system is stabilized. Pumping rate is set to 1 liter/min, cell pressure is set to 1000 psi, differential pressure is 20 psi and a temperature of 100 °F for the fluid and 150°F must be met beforehand. Once these conditions are reached, the acid is prepared and pumped.

The procedure followed is indicated below:

- 1- Apply a layer of Permatex Red Gasket Maker (Red RTV) around the rocks to enhance the seal between the sample and the cell (**Figure 16**).

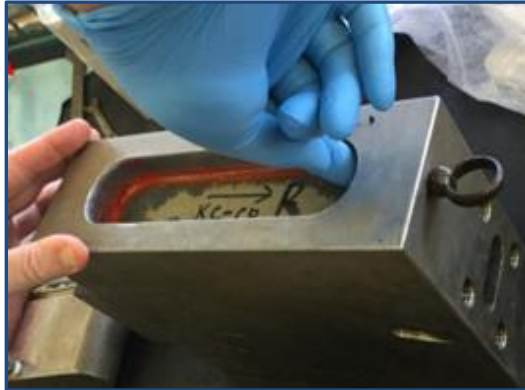


Figure 16. RTV Sealant around Sample

- 2- Attach the bottom flow insert and place the cell in the heavy duty frame. While still maintaining the shim in place, locate both side pistons in position, they must touch the bottom of the samples. The new pieces of metal installed will not let the pistons push the samples, so the problem of altering the width of the fracture is avoided. Lock the frame set up by tightening the long screws. Let the RTV dry for 24 hours.
- 3- Remove the shim, put on the heating jacket, set the temperature and wait for about six hours until rock reaches 150 °F.
- 4- Assembly the acid set up by connecting all the lines (inflow, outflow, front lines: cell pressure and leakoff pressure differential).

- 5- To reduce the handling of acid, for this experiments it was decided to measure the leakoff by weight, therefore a balance with a graduated beaker was installed in the outlet of the leakoff line.
- 6- Verify position of valves and houses where water and acid will be discarded from.
- 7- Set the pump flowrate to 1 liter/min.
- 8- Open the leakoff valve.
- 9- Start pumping water and verify if there are leaks in the system. If no leaks are present, slowly start increasing the cell pressure and the back up pressure to create the differential pressure from the beginning. It is recommended to start with as low as 100 psi. Repeat this step until a cell pressure of 1000 psi and a differential pressure of 20 psi is established.
- 10- Make sure that the leakoff has stabilized by weighting the volume of water from the leakoff line.
- 11- Prepare the acid mixture. For this project it is used 15% straight HCl and 15% HCl with the following additives: corrosion inhibitor, surfactant, non-emulsifying agent, scale inhibitor and acid gelling/friction reducer agent.
- 12- Prepare for acid pumping: Place outlet hose in waste barrel, place an empty bicker on the balance, close water valve and open acid valve.
- 13- Verify fluid pH from bleed off valve to start counting the acid time.
- 14- Once acid starts flowing on rock surface, record every minute the weight of the fluid from the leakoff line. Monitor the differential pressure at the same time.

- 15- When the experiment is completed, measure the total volume of leakoff acid collected. Close the acid valve and open the water valve.
- 16- Turn off the heating jacket and the heating tape.
- 17- Slowly, lower the cell and leakoff pressures.
- 18- Flush water in the system until a pH of 7 is reached (about 10 to 15 minutes).
- 19- Turn off the pump and close the water valve.
- 20- Disassemble the heavy duty acid frame. Take out the cell and remove all the sealant.
- 21- Carefully remove the sample from the cell, flush it with water and pat it dry.
- 22- Scan the surface of the sample in the profilometer by using the procedure explained before.

2.7 Fracture Conductivity Measurement

Conductivity experiments are performed to evaluate the remaining conductivity after an acid treatment is performed. To do so, different flow rates of nitrogen (4 flowrates were used in this research) are flowed in a closed system through the previously etched fracture. With each flowrate, the pressure drop across the fracture is recorded. This is repeated at different closure stress and by using Darcy's equation, conductivity is calculated.

The main components of the conductivity measurement apparatus are a stainless steel conductivity cell (API-RP-61), a load frame (model GCTS FRM4-100050S), a nitrogen tank, a gas flowmeter (max. capacity of 10 liter/min and precision of 0.001 liter/min), three pressure transducers, a backpressure regulator and a data acquisition system. Three ports in the conductivity cell are connected to the pressure transducers. The two transducers located towards the sides of the cell, measure the differential pressure across the fracture, while the other one located in the center provides the absolute cell pressure (**Figure 17**).

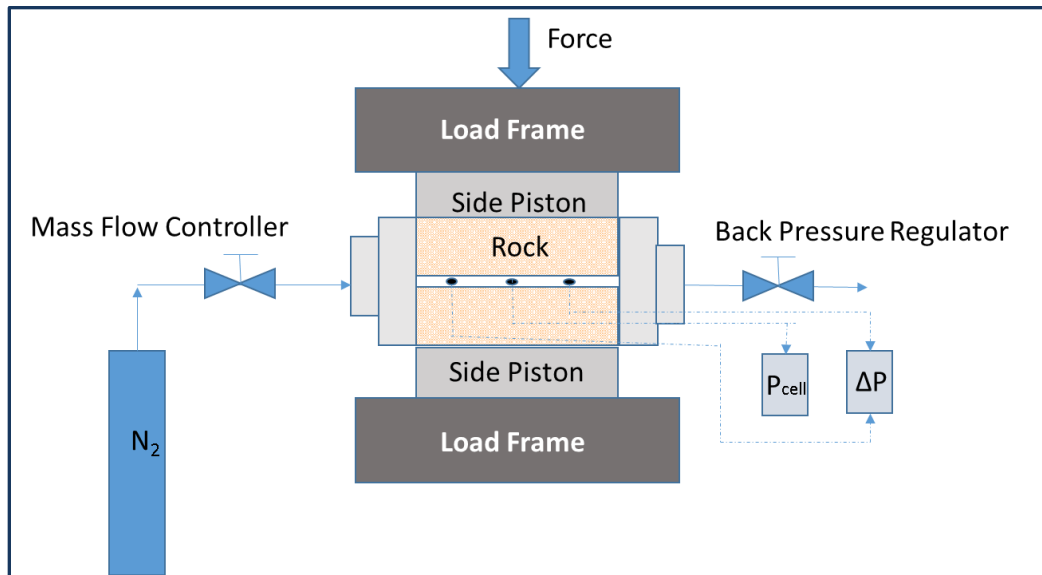


Figure 17. Conductivity Test Setup

Before starting the conductivity measurements, the sample must be prepared again. To do so, the RTV remaining from the acid test must be carefully removed. The mold used

for this experiment allows us to fully cover the sample with the silicon compound in one step. Later, it is placed in the oven for a period of 4 hours, to cure the RTV.

The procedure to perform the conductivity experiments is explained below:

- 1- Once the samples are taken out of the mold, cut squared shape sections of the RTV of about 0.5 in. These sections correspond to the location of the pressure transducer ports (**Figure 18**). They are located at 3 in, in the vertical direction and approximately 0.9 in, 3.5 in and 6.1 in in the horizontal direction (front of the sample). Fracture must be in direct contact with the pressure ports.



Figure 18. Sample Prepared for Conductivity Test

- 2- As in the previous step, cut similar sections on the sides of the sample, to allow for the entry and exit of nitrogen.
- 3- Clean sample from any debris and apply two layers of gas Teflon to prevent the leakage of nitrogen. The Teflon must be placed in between the cell ports in

the vertical direction and two more layers above and below the windows where the ports will be connected (**Figure 18**).

- 4- Apply a thin film of grease on the RTV, to ease the entrance of the sample in the cell.
- 5- Clean the conductivity cell and make sure that there are no fragments inside.
- 6- Press sample manually into the cell, and finish up introducing it with the hydraulic press. Make sure it is levelled off at all times. Sample must be placed in the same direction as for the acid test.
- 7- Place the sample horizontally in the load frame, introduce upper and lower pistons and the stabilizing sleeve. Align the cell in the equipment to ensure even distribution of force.
- 8- Turn on the GCTS UCT-1000 control box and once it shows the green lights, open the corresponding software and turn on the pump.
- 9- Plug in the Aalborg mass flowmeter, which must be warmed-up for a period of about 15 minutes (Zou, 2006).
- 10- Adjust the location of the GCTS piston until it applies a slight pressure on the sample.
- 11- Connect and tighten the lateral flow inserts.
- 12- Attach all the lines: differential pressure transducers, cell pressure transducer, gas inlet and outlet (**Figure 19**).

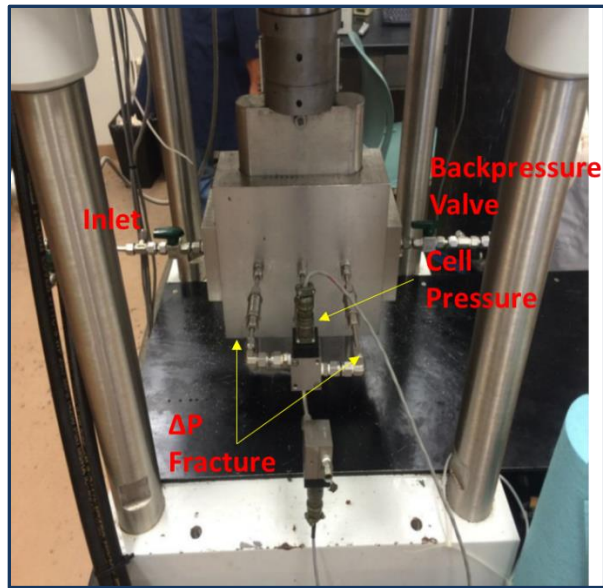


Figure 19. Lines Connected to Cell

- 13- Using the load frame, apply the initial loading pressure, which usually starts from 500 psi, but lower values can be used.
- 14- Tighten the top and bottom bleed bolt (two layers of Teflon must be wrapped in this bolt to prevent leakage).
- 15- Close the outlet valve and the bleed valve. Open the nitrogen root valve and slowly also open the system inlet valve. Flow nitrogen into the cell until it reaches a cell pressure of 30 psi, if the pressure does not build up it might indicate a leak in the system.
- 16- If there is suspicion of a leak, splash soapy water on the connections and around the top and bottom pistons, if there are bubbles that is an indication of a leak.

Tighten the proper fittings. If the leak persists, the experiment has to be stopped and reinstalled.

17- Apply the desired closure stress. Usually, 500 psi is the starting point.

18- When the system reaches the desired closure stress, take 4 flowrate readings by slowly opening the backpressure valve, while keeping the cell pressure between 25-30 psi. Record differential pressure, flowrates and cell pressure.

19- Repeat the procedure until the desired closure stress is reached or until the pressure drop in the fracture is exceeded by the pressure of the transducer.

20- When the test has finished, close the nitrogen tank and open the bleed valve to release the trapped gas. While doing this, don't exceed the rating of the flowmeter (10 lpm).

21- Disassemble the equipment by removing the flowlines and pressure transducers.

22- Remove the cell from the load frame and proceed to take out the sample by using the hydraulic jack.

The resultant conductivity is calculated using Darcy's Law equation and the Real Gas Law.

From Darcy's Law:

$$q = - \frac{KA}{\mu} \frac{dp}{dL} \quad (2.4)$$

And $q = v/A$ (2.5)

Substituting q :

$$-\frac{dp}{dL} = \frac{\mu v}{k} \tag{2.6}$$

Multiplying **Equation (2.6)** by the fluid density and rearranging:

$$-\frac{dp}{dL} * \rho_f = \frac{\mu v}{k} * \rho_f \tag{2.7}$$

From the fundamental concept of conservation of mass (continuity), density (ρ , kg/m³) is related to mass flow rate (W , kg/sec) and velocity (v , m/sec) by:

$$\rho = \frac{W}{Av} \tag{2.8}$$

Substituting **Equation 2.8** into **Equation 2.7**:

$$-\frac{dp}{dL} * \rho_f = \frac{\mu W}{kA} \tag{2.9}$$

Also, from the real gas law, the density is defined as:

$$\rho_f = \frac{pM}{ZRT} \quad (2.10)$$

Substituting **Equation 2.10** into **Equation 2.9**, yields:

$$-\frac{pM}{ZRT} * dp = \frac{\mu W}{kA} * dL \quad (2.11)$$

Integrating dp and dL in **Equation 2.11**:

$$-\frac{M}{ZRT} \int_1^2 p dp = \frac{\mu W}{kA} \int_1^2 dL \quad (2.12)$$

$$\frac{M}{ZRT} * \frac{(p_1^2 - p_2^2)}{2} = \frac{\mu W}{kA} * L \quad (2.13)$$

Calculating the fracture cross sectional area and the mass flowrate:

$$A = w_f * h_f \quad (2.14)$$

$$W = q * \rho_f \quad (2.15)$$

Substituting **Equations 2.14** and **2.15** into **Equation 2.13** and recognizing that $C_f = k_f * w_f$; the modified Darcy's law is:

$$\frac{(p_1^2 - p_2^2)M}{2ZRTL} = \frac{1}{C_f} \frac{q\rho\mu}{h_f} \quad (2.16)$$

From this equation; inlet pressure (p_1 , psi), outlet pressure (p_2 , psi), molecular weight (M , kg/mol), compressibility factor (Z , adim) temperature (T , K), fracture width (w_f , inch), fracture length (L , inch), gas flowrate (q , L/min), universal gas constant (R , J/mol.K), gas density (ρ , kg/m³), gas viscosity (μ , Pa.s).

The parameters in **Equation 2.16** are obtained from the conductivity test, they are: nitrogen flow rate (q), differential pressure across the fracture (ΔP) and the cell pressure (p_{cell}). p_1 and p_2 are calculated as a function of p_{cell} and Δp , considering that the inlet pressure (p_1) is equal to the pressure in the cell minus half of the total differential pressure and that the outlet pressure (p_2) is equal to the cell pressure plus half of the total Δp , the following expressions are generated:

$$p_1 = p_{cell} - \frac{\Delta p}{2} \quad (2.17)$$

$$p_2 = p_{cell} + \frac{\Delta p}{2} \quad (2.18)$$

To calculate conductivity, temperature is considered constant. **Table 1** shows the properties of the gas (nitrogen) as well as the values of the parameters used in **Equation 2.16**.

Table 1. Parameters Used for Fracture Conductivity

Parameter	Symbol	Value	Unit
Molecular Mass N ₂	M	0.028	Kg/kgmol
Fracture Width	h _f	1.650	inch
Compressibility Factor	Z	1	adim
Universal Gas Constant	R	8.314	J/mol.K
Differential Pressure Length	L	2.250	inch
Density of N ₂	ρ	1.161	Kg/m ³
Viscosity of N ₂	μ	1.759x10 ⁻⁵	Pa.s
Temperature	T	293.15	K

By plotting $\frac{(p_1^2 - p_2^2)M}{2ZRTL}$ in the y-axis and $\frac{q\rho\mu}{h_f}$ in the x-axis, fracture conductivity is

calculated as the inverse of the straight line slope (**Figure 20**).

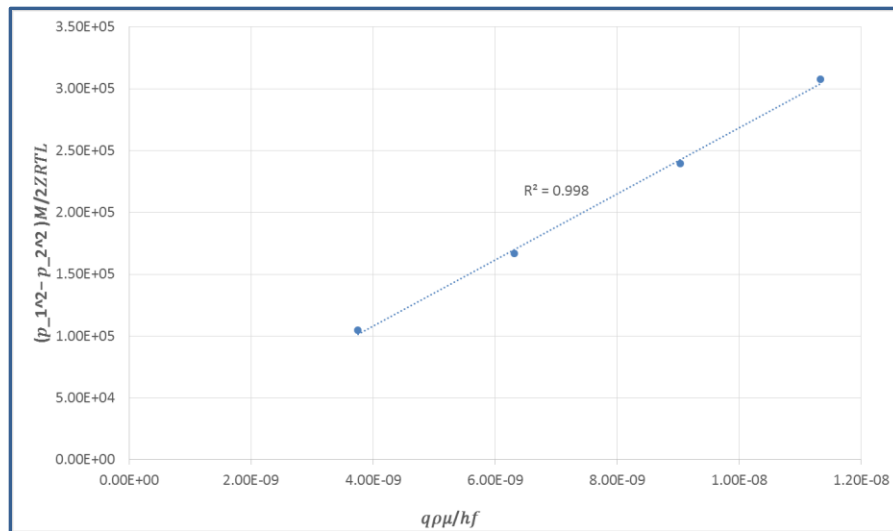


Figure 20. Computation of Fracture Conductivity from Four Data Points

2.8 Solubility Test

Solubility tests were performed to quantify the amount of insoluble material that resulted from the acid-rock reaction.

The procedure used to conduct the solubility tests is as follows:

- 1- Finely grind 10 grams of rock.
- 2- Place grinded rock in a container and slowly pour the acid mixture/straight 15% HCl. Make sure the acid contacts all the rock. As the rock dissolves, pour more acid until complete dissolution is achieved.
- 3- Pour the resulting mixture on filter paper, which had been previously weighted.
- 4- Flush through with approximately 100 ml of water to remove smaller insoluble particles that are still attached to the container and pour back in the filter paper.
- 5- Let dry completely (approximately two days at room temperature).
- 6- Weight and subtract the weight of the filter paper to obtain the mass of the insoluble material.

CHAPTER III

EXPERIMENTAL RESULTS AND DISCUSSION

In this research, the feasibility of acidizing soft carbonates such as Kansas Chalk and North Sea Chalk is studied. The influence of rock lithology, Brinell Hardness and the acid system used in the resultant conductivity is evaluated. A total of 11 Kansas Chalk outcrop and 4 North Sea Chalk cores samples were used in this investigation. Eight samples were acidized with straight 15% HCl, four samples were acidized with gelled 15% HCl with additives (corrosion inhibitor, surfactant, non-emulsifying agent, scale inhibitor and gelling agent), and three samples broke when they were being removed from the curing mold. **Table 2** presents a summary of the experimental conditions.

The experimental conditions are separated in three sections. The first section (sample #4 to sample #9) corresponds to the acid test conducted on Kansas Chalk at room temperature and with straight 15% HCl. The second section (sample #10 and sample #11), corresponds to the experiments done on Kansas Chalk but at higher temperature (150 °F for the rock and 100 °F for the fluid). In addition, sample#10 was acidized with straight 15% HCl and sample #11 was acidized with 15% HCl with additives. Lastly, the third section (sample #12 to sample #15) represents the experiments performed on North Sea Chalk cores. Three of these tests were conducted using 15% HCl with additives (samples #12, 13 and 14) and one of them (sample #15) was performed using 15% straight HCl.

The flowrate, cell pressure and differential pressure were kept constant for all the experiments at 1 liter/min, 1000 psi and 20 psi, respectively. Also, the fracture width was kept at 0.2 in.

Table 2. Experimental Conditions

Sample #	Sample Type	Sample ID	Rock Temp. (°F)	Fluid Temp. (°F)	Acid Type	Contact Time (min)	Flowrate (liter/min)	Fracture Width (in)
4	Kansas Chalk	KC-03-01	73	73	Straight 15% HCl	15	1	0.2
5	Kansas Chalk	KC-03-02	73	73	Straight 15% HCl	15	1	0.2
6	Kansas Chalk	KC-03-03	73	73	Straight 15% HCl	15	1	0.2
7	Kansas Chalk	KC-03-04	73	73	Straight 15% HCl	15	1	0.2
8	Kansas Chalk	KC-04-03	73	73	Straight 15% HCl	15	1	0.2
9	Kansas Chalk	KC-04-04	73	73	Straight 15% HCl	15	1	0.2
10	Kansas Chalk	KC-05-01	150	100	Straight 15% HCl	10	1	0.2
11	Kansas Chalk	KC-A+A	150	100	15% HCL + Addit.	15	1	0.2
12	North Sea Chalk	CP-05	150	100	15% HCL + Addit.	15	1	0.2
13	North Sea Chalk	CP-06	150	100	15% HCL + Addit.	15	1	0.2
14	North Sea Chalk	CP-07	150	100	15% HCL + Addit.	25	1	0.2
15	North Sea Chalk	CP-08	150	100	Straight 15% HCl	15	1	0.2

The similarities between Kansas Chalk and North Sea chalk are presented by several researchers. Haddadi (2009) shows a complete study of the porosity and permeability of the Kansas Chalk. He describes Kansas chalk as a weakly cemented and micritic (lime mud) carbonate. He states that this rock is similar to the North Sea Chalks, presenting a high porosity (30% to 50%) and low permeability (0.1 md to 3 md). In addition, Tang and Firoozabadi (2001) also describes the similarities between Kansas Chalk and the North Sea chalk in regard to porosity, permeability and calcite content.

The Kansas Chalk samples analyzed in this study had an average porosity of 31% and a Brinell Hardness that oscillates between 14000 to 17000 psi. For the North Sea cores, the porosity calculated with the pore volume method (equation 2.2), and the Brinell Hardness of the rock are shown in **Table 3**. The porosities calculated with the densities of the rock and the grain (Equation 2.3) were very similar ranging from 20% to 22%.

Brinell Hardness measurements were performed in four samples of Kansas Chalk and the four samples of North Sea cores. The Kansas Chalk samples had a Brinell Hardness number (BHN) that varied from 14000 psi (9.8 kgf/mm²) to 17000 psi (12 kgf/mm²). While the North Sea samples had a much higher Brinell Hardness number that varied from 25046 psi (17.6 kgf/mm²) to 28564 psi (20 kgf/mm²). From these results and according to the definition given by Gistau (1985), the Kansas Chalk samples can be regarded as “soft” chalk, while the North sea cores are regarded as “hard” chalks.

Table 3. Summary of Experimental Results

Sample #	Sample Formation	Porosity %	Brinell Hardness (psi)	Insoluble Residue from Solubility Test (%)	Acid Type	Contact Time (min)	Total Vol Etched (in ³)	Conductivity @ 500 psi	Observations
4	Kansas Chalk	31	14000 to 17000	None	Straight 15% HCl	15	3.59	2034	Rough surface
5	Kansas Chalk						-	211	Cracked
6	Kansas Chalk						3.29	-	Possible pressure ports blocked
7	Kansas Chalk						2.85	2600	Channels created
8	Kansas Chalk						6	143	Highest dissolved volume
9	Kansas Chalk						5.4	2631	Insoluble and hard material on surface
10	Kansas Chalk				10	-	-	Used for Leakoff control	
11	Kansas Chalk				HCl + Additiv.	15	0.5	Not measured	Used to observe reactivity with additives
12	North Sea Chalk	23	25046	23	HCl + Additiv.	15	-	-	Sample cracked during acid test
13	North Sea Chalk	25	27420	25	HCl + Additiv.	15	0.243	2063	-
14	North Sea Chalk	24	25814	25	HCl + Additiv.	25	0.76	46	Higher contact time used
15	North Sea Chalk	24	28564	28	Straight HCl	4	0.15	-	Acid brokethrough at minute 3

3.1 Acid Etching Results

A total of twelve acid etching tests were performed. Eight of them were carried out on Kansas Chalk and four of them on North Sea cores.

Experiments on samples #4 to #9 were performed at room temperature (73 °F) for both, the rock and the fluid. The contact time was 15 min at an injection rate of 1 liter/min. Samples #4, #5 and #6 showed similar volumes of rock dissolved. Sample #4 had a total volume of rock dissolved of 3.59 in³. Visual inspection of this sample after the acid test showed that the rock had some asperities distributed all over its surface. The 3D image of the scanned surface, shows high dissolution, but mostly uniform; indicated in the color palette (**Figure 21**). Sample #5 had two cracks on its upper surface (**Figure 22**). The upper side of the sample did not have much etching. Conversely, the lower side of the rock was differentially etched over the entire fracture surface. The surfaces of the fracture were not scanned because it had several cracks that would render erroneous results.

Samples #4 to #9 produced a very high leakoff rate caused by the lack of an effective sealing between the samples and the acid cell; reason why these measurements were considered not reliable.

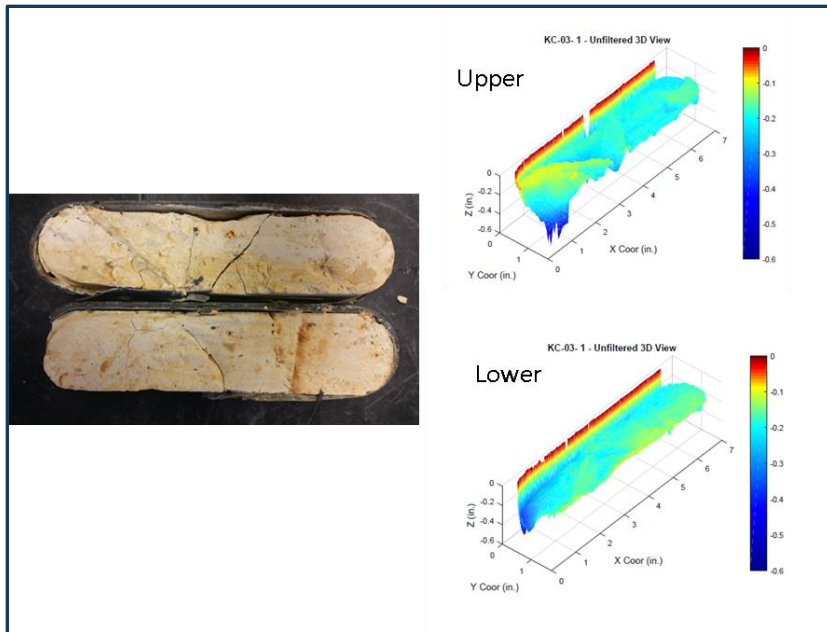


Figure 21. Surface Characterization of Sample #4. Right: Fracture Surface Scan from the Profilometer. Left: Picture of Acidized Fracture Surface



Figure 22. Acidized Surface of Sample #5

Sample #6 had a volume of rock dissolved of 3.29 in³, but the dissolution was mostly uniform over the fracture surface (**Figure 23**). No asperities were created during the acid injection. The fracture lacked pillars to prop it open when closure stress increases; therefore, the expected conductivity of this pattern is poor.

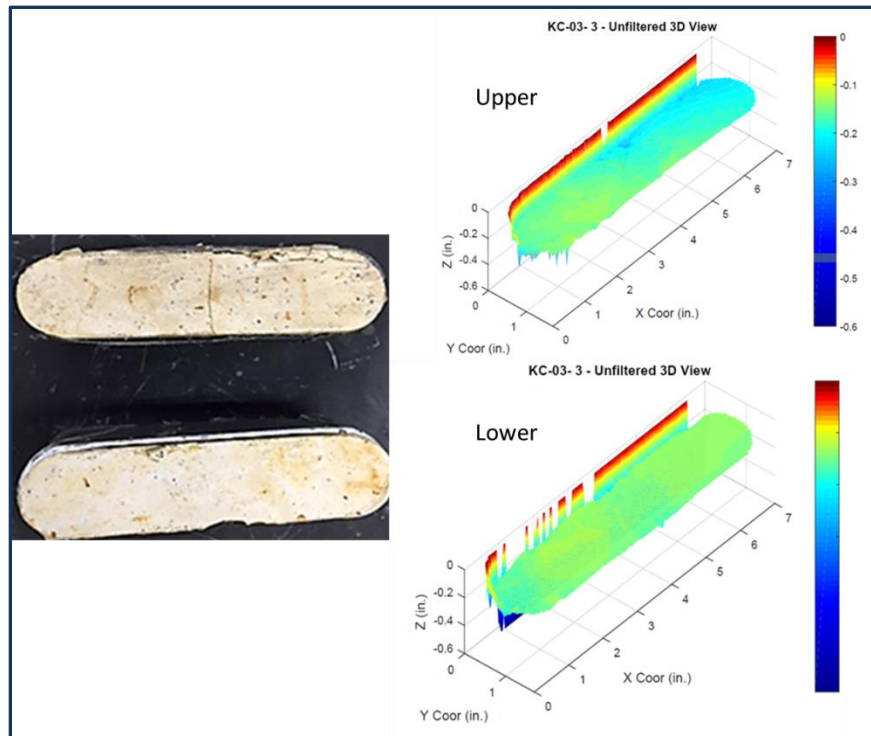


Figure 23. Surface Characterization of Sample #6. Right: Fracture Surface Scan from the Profilometer. Left: Picture of Acidized Fracture Surface

In the case of Sample # 7, it showed a different etching pattern than the previous experiments. Channels were observed on the surfaces of the fracture, which would be openings for fluid flow after deformation of the fracture caused by closure stress. From

the surface scan, it was observed the uneven rock dissolution on the fracture faces (**Figure 24**). The total volume of rock dissolved for sample #7 was 2.85 in³.

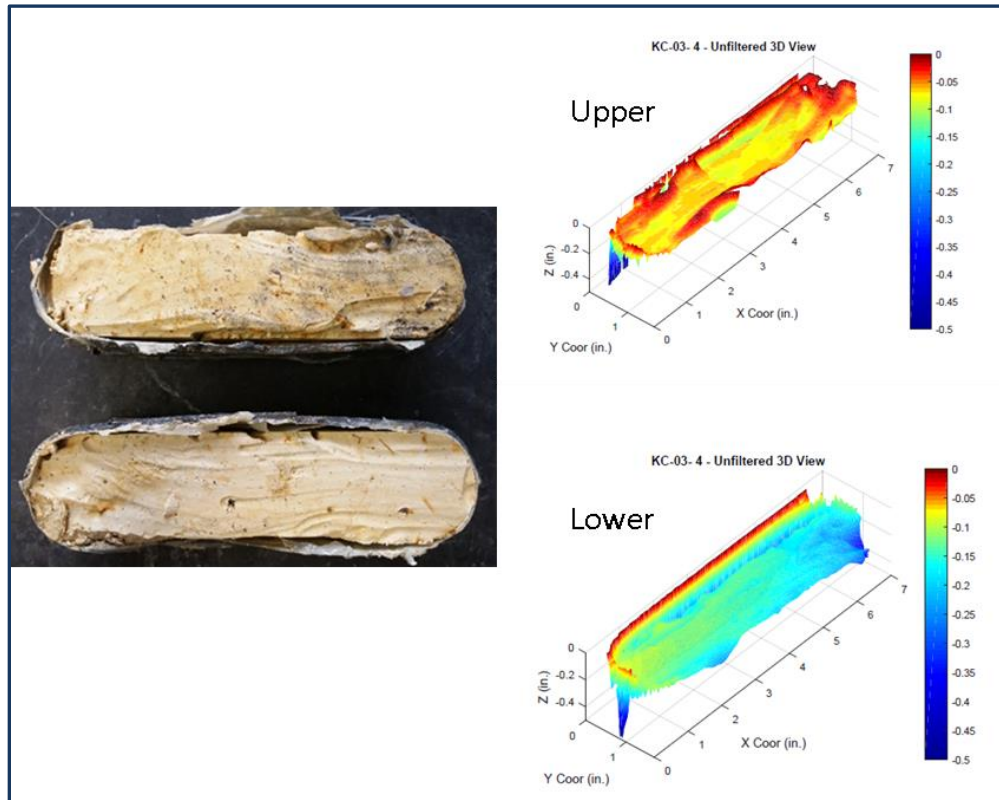


Figure 24. Surface Characterization of Sample #7. Right: Fracture Surface Scan from the Profilometer. Left: Picture of Acidized Fracture Surface

In the case of sample #8, it had a similar etching than sample #7, showing channels on the surfaces of the fracture (**Figure 25**). In addition, this sample showed some pits distributed over the surfaces. The volume of rock dissolved was the highest among all the samples tested, for a total of 6 in³. Following the color palette from the profilometer scan a deeper degree of dissolution is observed.

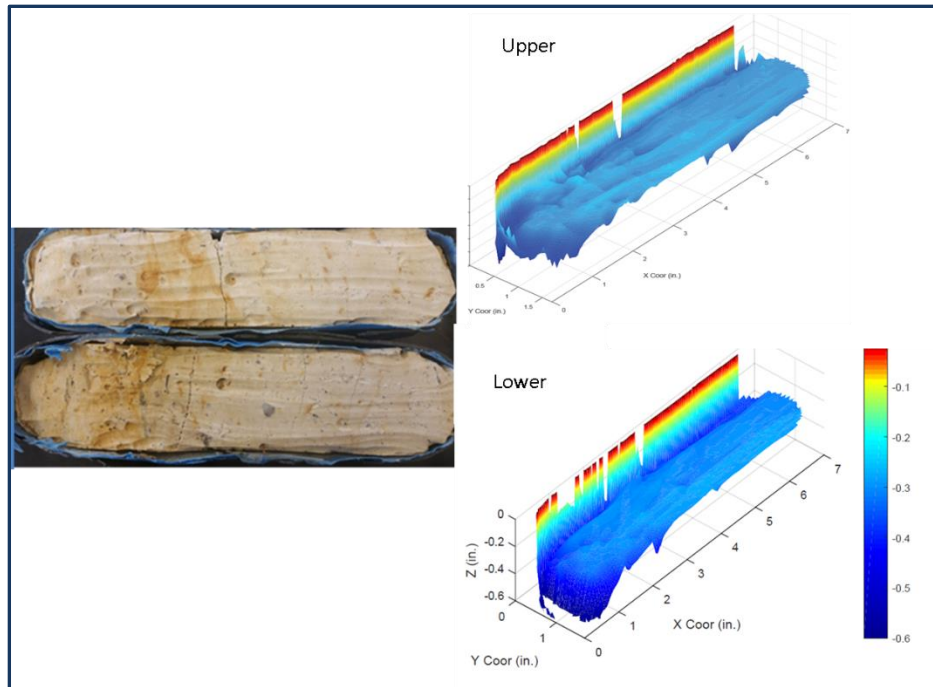


Figure 25. Surface Characterization of Sample #8. Right: Fracture Surface Scan from the Profilometer. Left: Picture of Acidized Fracture Surface

Sample #9 showed a scattered distribution of asperities and some channels on the fracture surfaces. It had the second highest volume of rock dissolved among all the samples, for a total of 5.4 in³. This sample had sections of an insoluble and hard material protruding on the fracture upper face (**Figure 26**).

In the case of sample #10, it was acidized for 10 minutes. This rock was not scanned on the profilometer nor did it have its conductivity measured. Its purpose was to establish a procedure to control the leakoff fluid that was flowing around the samples.

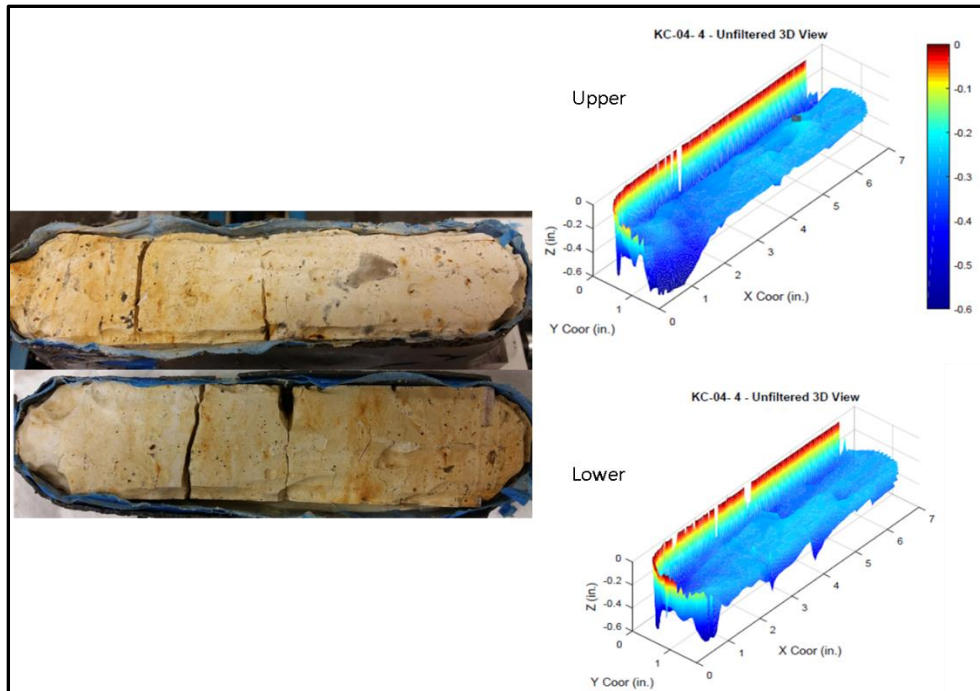


Figure 26. Surface Characterization of Sample #9. Right: Fracture Surface Scan from the Profilometer. Left: Picture of Acidized Fracture Surface

Sample #11 was acidized with 15% HCl with additives. The temperature was increased from room temperature conditions to 100 °F for the fluid and 150 °F for the rock. The acid contact time was 15 minutes. The purpose of acidizing this sample was to analyze its reaction to the acid, which now had these particular additives. The dissolution profile of Sample #11 is observed in **Figure 27**. This rock had a much lower volume of surface etched, when compared to previous experiments. The dissolution pattern is also more uniform all over the fracture surfaces; consequently, not much asperities developed during the acid test that could hold the fracture open. The total volume of rock dissolved for this sample was 0.5 in³.

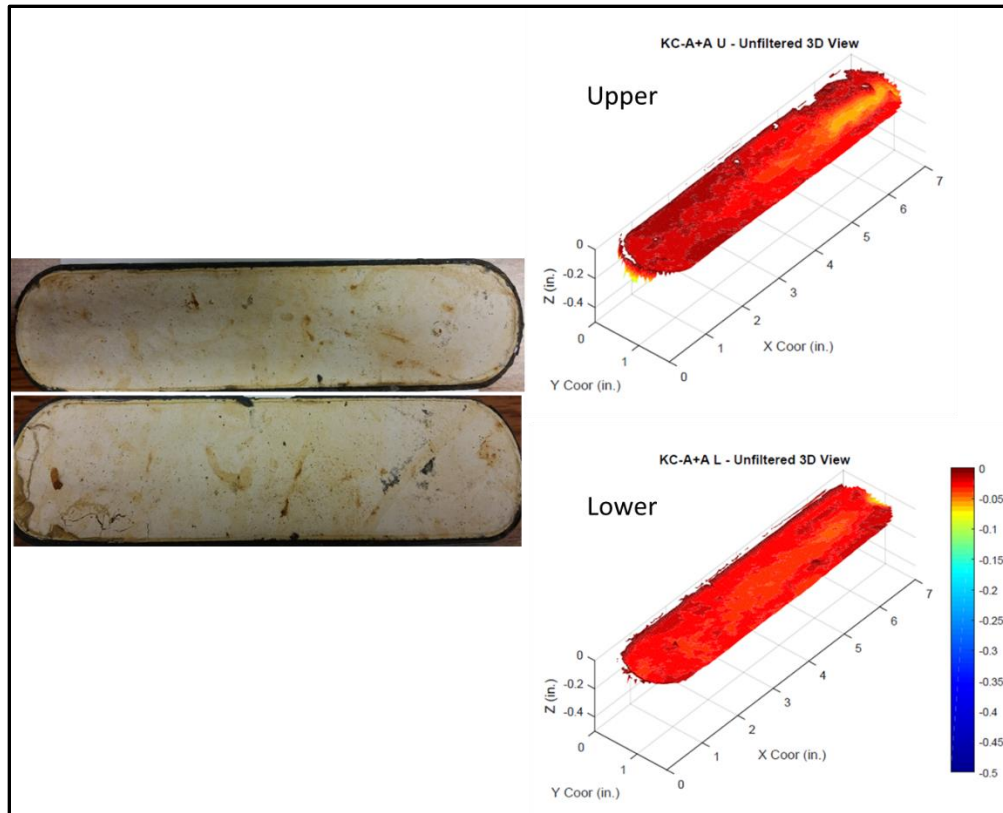


Figure 27. Surface Characterization of Sample #11. Right: Fracture Surface Scan from the Profilometer. Left: Picture of Acidized Fracture Surface

Sample #12 is a North Sea core. It was acidized at a fluid temperature of 100 °F and a rock temperature of 150 °F. The cell pressure, fracture width and flowrate remained unchanged. This sample developed a crack when it was extracted from the preparation mold; therefore the leakoff was not measured. In addition, after the acid test it was observed that hardly any etching had occurred on the surfaces of the rock. Though, some small wormholes were observed. These wormholes are the result of the enlargement of certain pores that initially receive a large amount of acid. A dark residue overall the fracture faces was present (**Figure 28**).



Figure 28. Acidized Fracture Surface of Sample # 12

In the case of sample #13, leakoff was measured, with all other test conditions. The total acid leakoff fluid collected was 210 ml (**Table 4**).

Some small wormholes were created on the surface of the rock, but not much differential etching was achieved. The total volume of rock dissolved was 0.243 in³. From the 3D surface scan, is possible to observe the dissolution profile of the fracture faces (**Figure 29**).

Table 4. Acid Leakoff Weight vs Time for Sample #13

Time (min)	Weight (g)
1	35.4
2	54.8
3	70.5
4	84.1
5	97.3
6	109.6
7	122.4
8	135.3
9	146.9
10	157.9
11	168.2
12	178
13	187
14	196
15	204.7

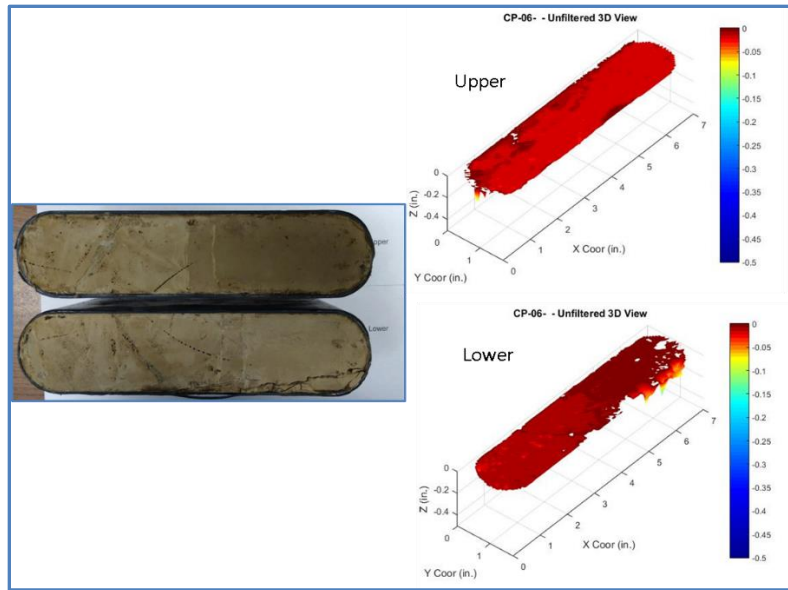


Figure 29. Surface Characterization of Sample #13. Right: Fracture Surface Scan from the Profilometer. Left: Picture of Acidized Fracture Surface

Due to the lack of differential etching obtained in the previous experiments with the North Sea cores, it was decided to increase the acid contact time. Thus, sample#14 acid contact time was increased from 15 minutes to 25 minutes, keeping the other experimental conditions unchanged. Leakoff fluid was also allowed. As acid was pumped through the fracture, the leakoff was quantified. At minute 12, a large increment of leakoff fluid occurred and the differential pressure decreased. This behavior was attributed at the creation of a crack or wormhole breakthrough. Despite the increment in the leakoff rate, just a total volume of 155 ml was collected (**Table 5**).

After the test, it was observed the creation of a film on the fracture surfaces. Uniform dissolution is perceived all over the surfaces of the rock (**Figure 30**). Regardless of the volume of rock dissolved (0.76 in^3 total), with this kind of pattern is impossible to

hold the fracture open when closure stress is applied; since there are no pillars to support it.

Table 5. Leakoff Measurement of Sample #14

Time (min)	Weight (g)	Δ Weight	Observations
1	6.6		System was stable
2	8.9	2.3	
3	11.1	2.2	
4	13.2	2.1	
5	15.1	1.9	
6	16.7	1.6	
7	18.4	1.7	
8	19.9	1.5	
9	22.6	2.7	
10	26.0	3.4	
11	27.9	1.9	
12	34.2	6.3	Leakoff increased Delta P decreased
13	44.6	10.4	
14	54.6	10	
15	64.1	9.5	
16	74.0	9.9	
17	84.9	10.9	
18	97.4	12.5	
19	107.4	10	
20	115.7	8.3	
21	123.7	8	
22	131.8	8.1	
23	139.7	7.9	
24	147.3	7.6	
25	154.9	7.6	

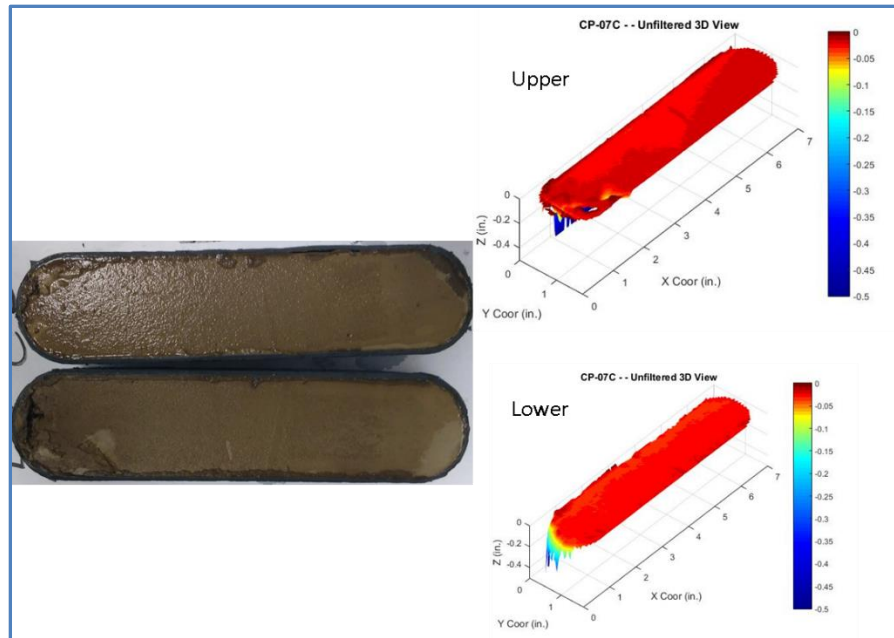


Figure 30. Surface Characterization of Sample #14. Right: Fracture Surface Scan from the Profilometer. Left: Picture of Acidized Fracture Surface

The last test was conducted on Sample #15. This rock was acidized with straight 15% HCl. The contact time of the acid was intended to be 15 minutes, but at minute 3, a sudden increase of the leakoff and a decrease in the differential pressure was observed; indicative of acid breaking through the rock (**Table 6**). At minute 4, the fluid was switched from acid to water, and it was flowed for 11 more minutes.

A thick layer of insoluble material was observed on the surface of the rock (**Figure 31**). Also, some small wormholes were scattered on the surfaces. The surfaces scan showed the lowest dissolution among all the samples, for a total of 0.15 in^3 ; which is influenced the short contact time.

Table 6. Leakoff vs Weight for Sample #15

Time (min)	Weight (gr)	ΔP (psi)	Fluid
1	8.2	24	Acid
2	17	19.6	
3	57.8	12.4	
4	118.2	12.2	
5	178	12.8	Water
6	-		
7	270	7.6	
8	310	6	
9	352	5.1	
10	394.3	4.8	
11	444.9	4.4	
12	495	5.6	
13	548.7	9.2	
14	603.4	7	
15	662	7	

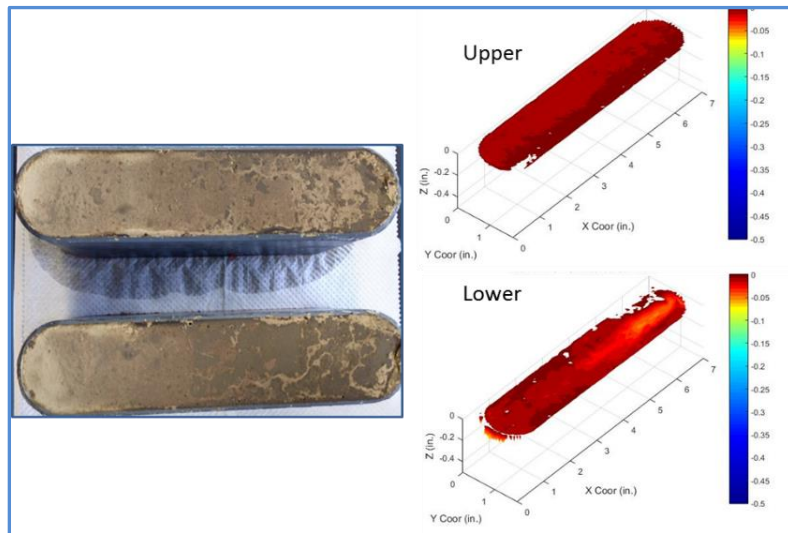


Figure 31. Surface Characterization of Sample #15. Right: Fracture Surface Scan from the Profilometer. Left: Picture of Acidized Fracture Surface

3.2 Solubility Tests and Analysis of Residual Material Results

All the North Sea core samples created a film on the fracture surfaces when they were exposed to the acid. To quantify the insoluble material, solubility tests were performed, following the procedure indicated in section 2.7. From these tests, a large amount of insoluble material was quantified (**Figure 32**). The results are summarized in **Table 7**.



Figure 32. Results from Solubility Test for Sample #12

From the solubility tests, is observed that the samples showed high amounts of insoluble material, being sample #15 the one with the largest amount of insoluble residue. The mineralogy of this samples might be responsible for these results.

Table 7. Results from Solubility Test, XRD, XRF and SEM Analysis

Test		Sample #	Results
Description	Number of Tests		
Insoluble Material, %	4	12	23
		13	25
		14	25
		15	28
XRD	2	12	46% Quartz
		13	15% Quartz
XRF	1	15	87% Quartz Clays
SEM	4	12	Quartz
		13	
		14	
		15	

This film was studied by performing X-Ray Diffraction (XRD), X-Ray Fluorescence (XRF) and Scanning Electron Microscope (SEM) analysis. **Table 7** shows the results of the tests performed in selected samples. These tests were carried out by a third party.

All the tests performed on either grinded rock before undergoing acid or residual material from the acid test, showed the presence of quartz. The XRF also showed the presence of some clays, which could explain the dark brown/greyish color of the residual material. An example of the SEM results is shown in **Figure 33**. The results from the XRF are shown in **Table 8**.

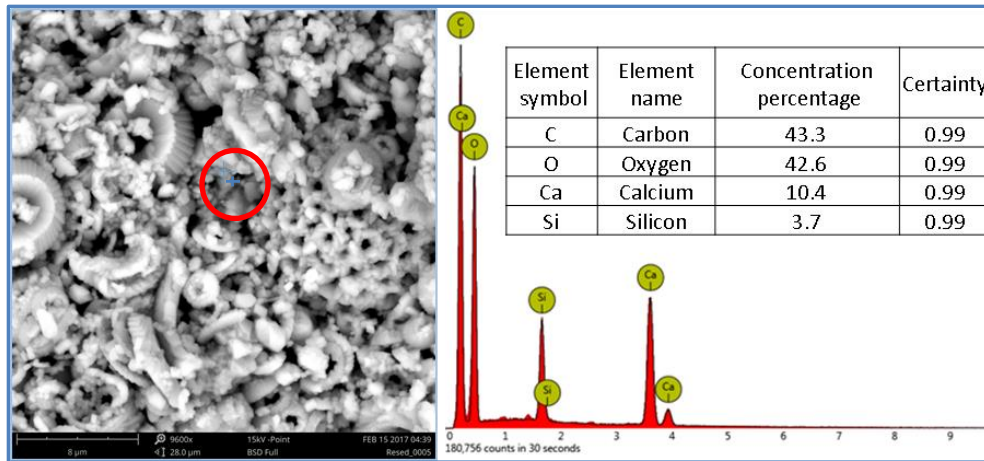


Figure 33. SEM Result from Sample #13

Table 8. XRF Results from Sample #15

Formula	Concentration, %
SiO ₂	85.6
Al ₂ O ₃	3.3
SO ₃	2.68
Fe ₂ O ₃	2.56
P ₂ O ₅	1.84
K ₂ O	1.23
Cl	0.925
CaO	0.742
Other	<1.1

3.3 Acid Fracture Conductivity Results

Acid fracture conductivity was measured for seven samples. Five of them were Kansas Chalk and two of them were North Sea cores. The results are presented in **Table 9**.

Table 9. Results from Acid Fracture Conductivity Test

Sample #	Conductivity @ 500 psi
4	2034
5	211
7	2600
8	143
9	2631
13 (North Sea)	2063
14 (North Sea)	46

The acid fracture conductivity as a function of closure stress for all the tested samples is shown in **Figure 34**.

The results indicate that fracture conductivity for the soft carbonate samples tested was not higher than 2600 md-ft at a closure stress of 500 psi and 796 md-ft at a closure stress of 1000 psi. A fast decline in conductivity with closure stress was seen in most samples. By comparing the slopes of each conductivity experiment, it was observed that the decline rate was similar. Sample #9 showed a slight slower decline, due to the presence of a hard material on the fracture surfaces which is believed that helped to sustain conductivity as closure stress increased. The conductivity of sample #4 and sample #7 are both high and very similar. They both had marked etching patterns, having sample #4 a rough etching pattern and sample #7 a channeling etching pattern. Sample #13 also showed an initial high fracture conductivity. Yet, an increase in the closure stress caused

an error in the reading of the differential pressure in the fracture conductivity setup and the conductivity could not be measured. Gas was not flowing through the fracture but around the sample.

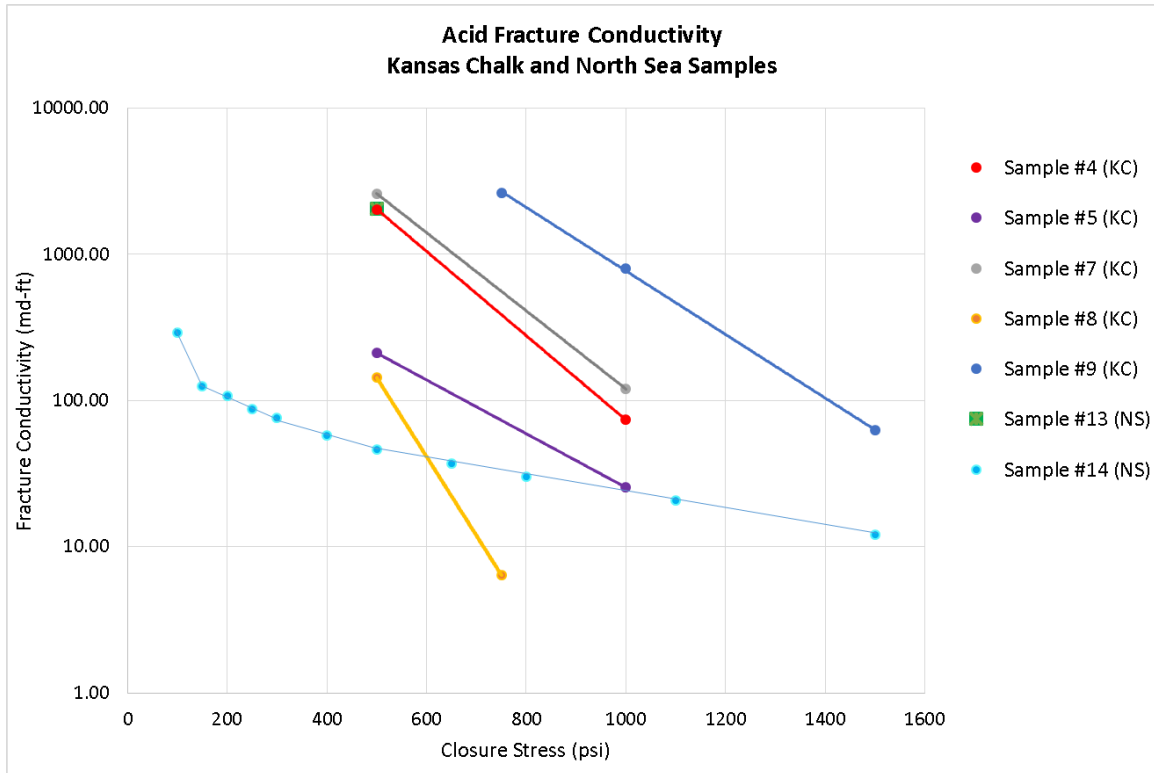


Figure 34. Acid Fracture Conductivity Behavior

Samples #5, #8 and #14 had the poorest fracture conductivity. The low result obtained in sample #5 was attributed to the lack of integrity of the sample. It had been glued together in different sections to undergo the fracture conductivity test; thus, this sample probably crushed during the test. In the case of sample #8, it had the highest

volume of rock dissolved. Also, it had channels and pits on the fracture surface. The mineralogy of this rock is believed to be playing an important role in the resultant conductivity. As for sample #14, its low fracture conductivity is credited to the increase in the acid contact time from 15 minutes to 25 minutes. Despite enhancing the volume of rock dissolved, it weakened the structure of the rock.

It was not possible to measure the conductivity for all the samples. Sample #6 conductivity measurement failed. The pressure transducer did not mark any change in reading. A blockage of the pressure ports with RTV or rock debris is believed to be responsible for this behavior. Samples #10 and #11 did not have their conductivity measured because they were used to control the leakoff and to observe the reaction of the rock to the acid system with additives. Sample #12 was the first sample from the North Sea cores to undergo acid fracture conductivity. It was also the first sample that showed the residual material on the fracture surfaces. This sample was acidized two times to observe if the insoluble residue was caused by the acid. Therefore, no conductivity measurement was done. In the case of sample #15, the acid test was stopped after just 4 minutes because of a sudden increase in the leakoff fluid. Not a representative value of conductivity would be taken from this experiment.

3.4 Discussion of Results

Comparing the volume of rock dissolved among the samples acidized during 15 minutes (**Table 10**), it was observed that the Kansas Chalk had a much higher volume of

rock dissolved than the North Sea cores. The fact that the Kansas Chalk did not render any insoluble residue, enhanced the volume of rock etched. In addition, it was observed that an increase in the contact time increased the volume of rock dissolved for the North Sea cores, yet it affected the fracture conductivity.

The results clearly show the effect that the acid additives have on rock dissolution. In the acid mixture for samples #11 to #14, a gelling agent was used. Usually, they are added to allow greater penetration. The gelling agent increases the viscosity of the fluid and slow down the diffusion of H^+ from the bulk solution to the surface of the rock, thus decreasing the dissolution of the rock by the acid.

In the North Sea cores, no differential etching was achieved. Neither increasing the contact time of the acid nor using straight acid promoted the uneven dissolution of the surfaces of the fractures.

Table 10. Summary Results from Acid Fracture Conductivity Experiments

Sample #	Sample Formation	Acid Type	Contact Time (min)	Temperature Rock/Fluid (°F)	Total Vol Etched (in ³)	Conductivity @ 500 psi
4	Kansas Chalk	Straight HCl	15	73/73	3.59	2034
5	Kansas Chalk		15	73/73	-	211
6	Kansas Chalk		15	73/73	3.29	-
7	Kansas Chalk		15	73/73	2.85	2600
8	Kansas Chalk		15	73/73	6	143
9	Kansas Chalk		15	73/73	5.4	2631 l
10	Kansas Chalk		10	73/73	-	-
11	Kansas Chalk	HCl + Additiv.	15	150/100	0.5	-
12	North Sea Chalk	HCl + Additiv.	15	150/100	-	-
13	North Sea Chalk	HCl + Additiv.	15	150/100	0.243	2063
14	North Sea Chalk	HCl + Additiv.	25	150/100	0.76	46
15	North Sea Chalk	Straight HCl	4	150/100	Acid brokethrough at min 3	-

The formation of a layer of insoluble residue on the surfaces of the fractures is believed to be responsible for this lack of reaction. The analysis of the residual material showed the presence of silicates and clays, which do not react to HCl. XRD, XRF and SEM analysis, agreed with the results obtained from other researchers that studied this formation (Gennaro et al., 2012, Melendez, 2007, Jakobsen et al., 2000, Simon et al., 1982, Maliva and Dickson, 1992, Lindgreen and Jakobsen, 2012). They also identified the presence of insoluble material containing quartz and clay minerals. From the XRF, a large percentage of quartz was found, with some clays present. The XRF analysis has the capability of reading ultrafine particles, such as nano-quartz and clay minerals, (Lindgreen and Jakobsen, 2012); this could explain the large amount of quartz found in this sample with this analysis technique.

Furthermore, there seems to be a correlation between the volume of insoluble material found and the Brinell Hardness of the samples (**Figure 35**); as the content of insoluble material increased, so did the Brinell Hardness. Additional testing is required to determine its veracity.

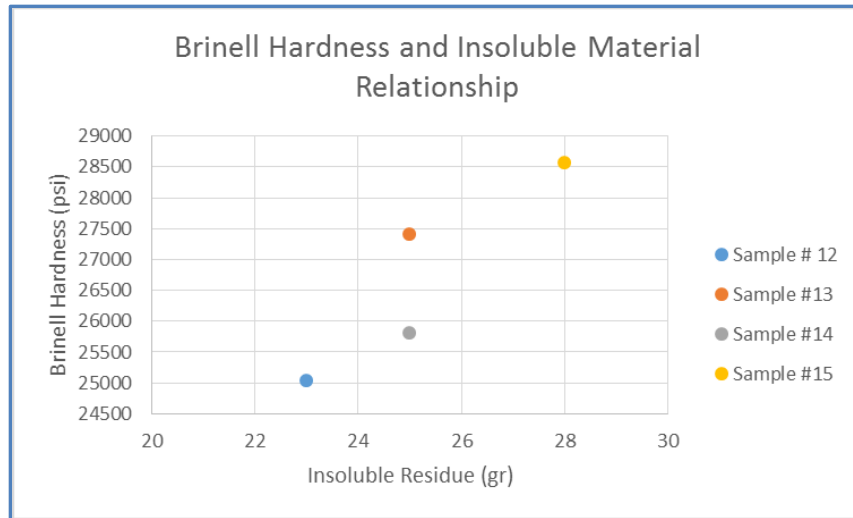


Figure 35. Brinell Hardness Relationship with Insoluble Material

3.5 Comparison of Kansas Chalk and North Sea Chalk with Indiana Limestone

The type of formation has a strong impact in the differential etching and the resultant conductivity. Formation characteristics, such as porosity, permeability, rock strength, and mineral distribution affect the reaction rate between the fluid and the rock; consequently, impacting rock dissolution and the resultant conductivity.

In general, chalk is a special form of limestone, which is mainly composed of calcium carbonate; reason why it is highly soluble in HCl. On the other hand, limestone can contain up to 50% of impurities making it much harder than chalk and also affecting its solubility.

Several researchers have investigated the relationship between the formation type and rock strength on fracture conductivity (Nierode and Kruk, 1973, Gong et al., 1998, Gomaa and Nasr-El-Din, 2009, Melendez et al., 2007) performed rock strength measurements and acid fracture conductivity experiments on Indiana limestone, among other rock types. In her experiments, she used gel acid 15% HCl at 175 °F. The reported rock strength values oscillated between 28,300 psi and 39,200 psi. Furthermore, Melendez (2007) obtained a volume of rock dissolved of about 0.7 in³ for a 20 minute of acid contact time.

In this research, the rocks used were softer, especially the Kansas chalk. It had a very low strength that varied from 14,000 psi to 17,000 psi, while North Sea chalk strength fluctuated between 25,000 to 28,500 psi.

The conductivity response of the Indiana limestone reported by Melendez (2007) differs with the conductivity response of the studied Kansas and North Sea chinks. Melendez (2007) found that for Indiana limestone, as contact time increased, the conductivity was dominated by a channeling pattern on the fracture surface. In addition, the author stated that in the lack of channels, the strength of the created pillars were responsible for maintaining the fracture open. She reported conductivity values of 3264 md-ft for a closure stress of 1000 psi, for samples acidized for 30 minutes and a conductivity of 1208 md-ft for samples acidized for 20 min. On the other hand, our results for the conductivity response measured for the Kansas and the North Sea chinks were poorer. At 500 psi of closure stress, the highest conductivity value achieved was 2631 md-ft, for a contact time of 15 minutes in the Kansas chalk. These lower values of conductivity

are expected for a rock that is much softer than Indiana limestone. Moreover, for the North Sea cores, the conductivity response was impaired by the lack of differential etching on the surfaces of the samples. Neither of the acid systems used was capable of enhancing the differential etching of the rock. The mineral composition of the rock showed an abundance of insoluble material that are believed to be impairing the dissolution on the surface of the rock.

CHAPTER IV

CONCLUSIONS AND RECOMMENDATIONS

4.1 Conclusions

Acid fracture conductivity experiments were carried out on Kansas Chalk outcrops and North Sea cores. Their interaction with acid and the resulting conductivity was examined. The conclusions made after the tests, are presented.

- 1- The addition of additives to the HCl reduced the volume of rock etched. The reaction rate of the acid decreased when additives were added to the fluid.
- 2- Highest volumes of rock dissolved did not render the highest conductivity. The lack of strength of the rock played a major role.
- 3- Increasing the contact time in the North Sea cores from 15 minutes to 25 minutes, did not enhance conductivity, possibly caused by the mostly even etching of the fracture face and the weakening of the rock structure.
- 4- The dissolution of the studied North Sea cores in HCl was limited. As the acid reacted with the rock, a film formed on its surface and prevented the reaction between the HCl and the chalk.
- 5- The North Sea cores never developed a rough surface, making impossible to achieve and sustain conductivity.

- 6- Acid fracture conductivity experiments on soft carbonates cannot be performed using carbonate samples whose thickness is less than 1.2 inches.

4.2 Recommendations

- 1- With the North Sea cores, analyze the feasibility of using another stimulation method, such as a fracturing treatment with proppants, to increase conductivity. Acid fracturing did not create much differential etching; therefore, the created conductivity was poor.

REFERENCES

Abass, H. H., Al-Mulhem, A. A., Alqam, M. H. et al. 2006. Acid Fracturing or Proppant Fracturing in Carbonate Formation? A Rock Mechanics View. SPE Annual Technical Conference and Exhibition, 24-27 September, San Antonio, Texas, USA.

American Petroleum Institute. 1989. Recommended Practices for Evaluating Short Term Proppant Pack Conductivity. API RP-61, Washington DC, USA.

Anderson, M., Fredrickson, S. . 1989. Dynamic Etching Tests Aid Fracture-Acidizing Treatment Design. SPE Production Engineering 4 (04): 443-449.

Antelo, L. F., Zhu, D., Hill, A. D. 2009. Surface Characterization and its Effect on Fracture Conductivity in Acid Fracturing. SPE Hydraulic Fracturing Technology Conference, 19-21 January, The Woodlands, Texas, USA.

Bazin, B., Roque, C., Chauveteau, G. et al. 1999. Acid Filtration Under Dynamic Conditions To Evaluate Gelled Acid Efficiency in Acid Fracturing. SPE Journal 4 (04): 360-367.

Beg, M., Kunak, A. , Gong, M. et al. 1996. A Systematic Experimental Study of Acid Fracture Conductivity. SPE Formation Damage Control Symposium, 14-15 February, Lafayette, Louisiana, USA.

Bocaneala, B., Barrett, C., Holland, B. et al. 2015. The Evolution of Completion Practices and Reservoir Stimulation Techniques in the North Sea. SPE Offshore Europe Conference and Exhibition, 8-11 September, Aberdeen, Scotland, UK.

Cook, C. , Brekke, K. 2004. Productivity Preservation via Hydraulic Propped Fractures in the Eldfisk North Sea Chalk Field. SPE Reservoir Evaluation & Engineering 7 (02): 105-114.

Cook, C., Brekke, K. 2002. Productivity Preservation via Hydraulic Propped Fractures in the Eldfisk North Sea Chalk Field. International Symposium and Exhibition on Formation Damage Control, 20-21 February, Lafayette, Louisiana, USA.

Deng, J., Mou, J., Hill, A. et al. 2011. A New Correlation of Acid-Fracture Conductivity Subject to Closure Stress. SPE Production & Operations 26 (01): 9-17.

Gennaro, M. , Wonham, J., Saalen, G. et al. 2012. Characterization of Dense Zones within Danian Chalks of the Ekofisk Field, Norwegian North Sea. Petroleum Geoscience 19: 39-64.

Gistau, M. 1985. Stimulation Methods and Practices on Chalk Reservoirs. Chalk Symposium, Stavenger, Norway.

Gomaa, A., Nasr-El-Din, H. 2009. Acid Fracturing: The Effect of Formation Strength on Fracture Conductivity. SPE Hydraulic Fracturing Technology Conference, 19-21 January, The Woodlands, Texas, USA.

Gong, M., Lacote, S., Hill, A. . 1998. A New Model of Acid Fracture Conductivity Based on Deformation of Surface Asperities. SPE Formation Damage Control Conference, 18-19 February, Lafayette, Louisiana, USA.

Haddadi, D. 2009. An Investigation on Permeability and Porosity Evolution of Kansas Chalk Under In-situ Conditions. Master of Science, University of Stavenger, Stavenger, Norway.

Jakobsen, F., Lindgreen, H., Springer, N. 2000. Precipitation and Flocculation of Spherical Nanosilica in North Sea Chalk. Geological Survey of Denmark and Greenland 35: 175-184.

Lindgreen, H. , Fallick, A., Jakobsen, F. et al. 2012. The Tight Danian Ekofisk Chalk Reservoir Formation in the South Arne Field, North Sea: Mineralogy and Porosity Properties. Journal of Petroleum Geology 35 (3): 291-309.

Lindgreen, H. , Jakobsen, F. 2012. Nano quartz in North Sea Danian Chalk. Geological Survey of Denmark and Greenland 38 (1): 73-82.

Mader, D. 1989. Hydraulic Proppant Fracturing and Gravel Packing, Chap. 4, 333-657. New York, Elsevier.

Malagon, C. 2006. The Texture of Acidized Fracture Surfaces-Implications for Acid Fracture Conductivity. Master of Science, Texas A&M University, Texas, USA.

Maliva, R., Dickson, J. 1992. Microfacies and Diagenetic Controls of Porosity in Cretaceous/Tertiary Chalks, Eldfisk, Norwegian North Sea. American Association of Petroleum Geology 76 (11): 1825-1838.

Mancillas, G., Matson, R., Ziara, B. 1976. Stimulation of the Ekofisk. SPE Annual Fall Technical Conference and Exhibition, 3-6 October, New Orleans, Louisiana, USA.

Melendez, M. 2007. The Effects of Acid Contact Time and Rock Surfaces on Acid Fracture Conductivity. Master of Science, Texas A&M University, Texas, USA.

Melendez, M., Pournik, M., Zhu, D. et al. 2007. The Effects of Acid Contact Time and the Resulting Weakening of the Rock Surfaces on Acid Fracture Conductivity. European Formation Damage Conference, 30 May-1 June, Scheveningen, The Netherlands.

Nierode, D., Kruk, K. . 1973. An Evaluation of Acid Fluid Loss Additives Retarded Acids, and Acidized Fracture Conductivity. Fall Meeting of the Society of Petroleum Engineers of AIME, 30 September-3 October, Las Vegas, Nevada, USA.

Nierode, D., Williams, B. , Bombardieri, C. . 1972. Prediction of Stimulation From Acid Fracturing Treatments. Journal of Canadian Petroleum Technology 11 (04).

Pollastro, R., Martinez, Carl. 2012. Fine-Grained Deposits and Biofacies of the Cretaceous Western Interior Seaway: Evidence of Cyclic Sedimentary Processes. The Society of Economic Paleontologists and Mineralogists 4.

Pournik, M. 2008. Laboratory Scale Fracture Conductivity Created by Acid Etching. Doctor of Philosophy, Texas A&M University, Texas, USA.

Pournik, M., Gomaa, A., Nasr-El-Din, H. 2010. Influence of Acid-Fracture Fluid Properties on Acid-Etched Surfaces and Resulting Fracture Conductivity. SPE International Symposium and Exhibiton on Formation Damage Control, 10-12 February, Lafayette, Louisiana, USA.

Rabie, A., Nasr-El-Din, H. 2015. Effect of Acid Additives on the Reaction of Stimulating Fluids During Acidizing Treatments. SPE North Africa Technical Conference and Exhibition, 14-16 September, Cairo, Egypt.

Simon, D., Coulter, G., King, George et al. 1982. North Sea Chalk Completions- A Laboratory Study. Journal of Petroleum Technology 34 (11): 2531-2536.

Snow, S., Hough, E. . 1988. Field and Laboratory Experience in Stimulating Ekofisk Area North Sea Chalk Reservoirs. SPE Annual Technical Conference and Exhibition, 2-5 October, Houston, Texas, USA.

Tang, G., Firoozabadi, A. 2001. Effect of Pressure Gradient and Initial Water Saturation on Water Injection in Water-Wet and Mixed-Wet Fractured Porous Media. SPE Reservoir Evaluation & Engineering 04 (06): 516-524.

Van der Voet, Eva. 2015. Geological Evolution of the Chalk Group in the Northern Dutch North Sea. Master of Science, Amsterdam University, Amsterdam.

Van Domelen, M. , Ford, W. , Chiu, T. . 1992. An Expert System for Matrix Acidizing Treatment Design. SPE Annual Technical Conference and Exhibition, 4-7 October, Washington, D.C., USA.

Zou, C. 2006. Development and Testing of an Advanced Acid Fracture Conductivity Apparatus. Master of Science, Texas A&M University, Texas, USA.